frontiers in Marine Science

ORIGINAL RESEARCH
published: 09 June 2021
doi: 10.3389/fmars.2021.661158

Planktic Foraminiferal and Pteropod Contributions to Carbon Dynamics in the Arctic Ocean (North Svalbard Margin)

Griselda Anglada-Ortiz[1], Katarzyna Zamelczyk[2], Julie Meilland[3], Patrizia Ziveri[4,5], Melissa Chierici[6], Agneta Fransson[2] and Tine L. Rasmussen[1]*

[1] Centre for Arctic Gas Hydrate, Environment and Climate (CAGE), Department of Geosciences, UiT The Arctic University of Norway, Tromsø, Norway, [2] Oceans and Sea Ice, Norwegian Polar Institute (NPI), Tromsø, Norway, [3] MARUM Center for Marine Environmental Sciences, University of Bremen, Bremen, Germany, [4] Institute of Environmental Science and Technology (ICTA), Autonomous University of Barcelona, Barcelona, Spain, [5] ICREA, Catalan Institution for Research and Advanced Studies, Barcelona, Spain, [6] Oceanography and Climate, Institute of Marine Research (IMR), Tromsø, Norway

Planktic foraminifera and shelled pteropods are some of the major producers of calcium carbonate ($CaCO_3$) in the ocean. Their calcitic (foraminifera) and aragonitic (pteropods) shells are particularly sensitive to changes in the carbonate chemistry and play an important role for the inorganic and organic carbon pump of the ocean. Here, we have studied the abundance distribution of planktic foraminifera and pteropods (individuals m^{-3}) and their contribution to the inorganic and organic carbon standing stocks (μg m^{-3}) and export production (mg m^{-2} day^{-1}) along a longitudinal transect north of Svalbard at 81° N, 22–32° E, in the Arctic Ocean. This transect, sampled in September 2018 consists of seven stations covering different oceanographic regimes, from the shelf to the slope and into the deep Nansen Basin. The sea surface temperature ranged between 1 and 5°C in the upper 300 m. Conditions were supersaturated with respect to $CaCO_3$ ($\Omega > 1$ for both calcite and aragonite). The abundance of planktic foraminifera ranged from 2.3 to 52.6 ind m^{-3} and pteropods from 0.1 to 21.3 ind m^{-3}. The planktic foraminiferal population was composed mainly of the polar species *Neogloboquadrina pachyderma* (55.9%) and the subpolar species *Turborotalita quinqueloba* (21.7%), *Neogloboquadrina incompta* (13.5%) and *Globigerina bulloides* (5.2%). The pteropod population was dominated by the polar species *Limacina helicina* (99.6%). The rather high abundance of subpolar foraminiferal species is likely connected to the West Spitsbergen Current bringing warm Atlantic water to the study area. Pteropods dominated at the surface and subsurface. Below 100 m water depth, foraminifera predominated. Pteropods contribute 66–96% to the inorganic carbon standing stocks compared to 4–34% by the planktic foraminifera. The inorganic export production of planktic foraminifera and pteropods together exceeds their organic contribution by a factor of 3. The overall predominance of pteropods over foraminifera in this high Arctic region during the sampling period suggest that inorganic standing stocks and export production of biogenic carbonate would be reduced under the effects of ocean acidification.

Keywords: inorganic and organic carbon pump, planktic calcifiers, standing stocks, export production, Atlantification

OPEN ACCESS

Edited by:
Sunil Kumar Singh,
Physical Research Laboratory, India

Reviewed by:
Arun Deo Singh,
Banaras Hindu University, India
Sushant Naik,
National Institute of Oceanography (CSIR), India

****Correspondence:***
Griselda Anglada-Ortiz
griselda.a.ortiz@uit.no

Specialty section:
This article was submitted to Marine Biogeochemistry, a section of the journal Frontiers in Marine Science

Received: *30 January 2021*
Accepted: *05 May 2021*
Published: *09 June 2021*

Citation:
Anglada-Ortiz G, Zamelczyk K, Meilland J, Ziveri P, Chierici M, Fransson A and Rasmussen TL (2021) Planktic Foraminiferal and Pteropod Contributions to Carbon Dynamics in the Arctic Ocean (North Svalbard Margin). Front. Mar. Sci. 8:661158. doi: 10.3389/fmars.2021.661158

INTRODUCTION

The increasing atmospheric uptake of CO_2 by the surface ocean is changing the seawater carbonate chemistry by reducing the pH, the carbonate ion concentration and the calcium carbonate ($CaCO_3$) saturation state (Ω). This process, referred to as ocean acidification, may have irreversible consequences for marine calcifiers, such as planktic foraminifera and shelled pteropods. Ocean acidification can cause reduced calcification rates (Fabry, 2008; Moy et al., 2009; Manno et al., 2017; Schiebel et al., 2017) or dissolution or damage of the shells in case of $CaCO_3$ undersaturation ($\Omega < 1$) (Peck et al., 2018) and references therein. Due to the sensitivity of their shells, planktic foraminifera and pteropods are used as biological indicators of ocean acidification [e.g., Orr et al. (2005), Fabry et al. (2008), Moy et al. (2009), Bednaršek et al. (2012c)]. Moreover, they are important for the carbonate budget and changes in their distribution patterns and productivity can alter the buffer capacity of the ocean (Schiebel, 2002; Ziveri et al., 2007; Langer, 2008; Bednaršek et al., 2012a; Salter et al., 2014; Buitenhuis et al., 2019).

Planktic foraminifera are unicellular protists with shells made of calcite. They mainly occur in the upper 300 m of the water column. Due to their sensitivity to environmental conditions and the excellent preservation patterns in sedimentary geological records, they are extensively used as proxies to reconstruct past physical and chemical parameters of the upper ocean (Katz et al., 2010). However, only few studies have investigated their sensitivity to present and past ocean acidification (Moy et al., 2009; Roy et al., 2015; Davis et al., 2017; Fox et al., 2020).

Shelled pteropods are holoplanktic gastropods with a shell made of aragonite. They live in the upper water column. Aragonite is the most soluble form of $CaCO_3$ and therefore more vulnerable to water carbonate chemistry changes than calcite (Bednaršek et al., 2012b; Manno et al., 2017). The pteropod species *Limacina helicina* has shown damage of the aragonite shell even in supersaturated waters with a Ω_{AR} of 1.5 (Bednaršek et al., 2014, 2019).

Planktic foraminifera and pteropods are the major zooplankton producers of $CaCO_3$ and a key component of the ocean carbon cycle (Guinotte and Fabry, 2008). Besides coccolithophores (unicellular phytoplankton), they have an important role in exporting carbon from the surface to the deep ocean. In particular, shelled pteropods contribute to the biological carbon pump exporting organic carbon (particulate organic carbon) through formation of aggregates and fecal pellets (Manno et al., 2018) and references therein. Planktic foraminifera and shelled pteropods also contribute to the opposite process known as the carbonate counter pump. Through the calcification of their inorganic shells, the carbonate counter pump results in producing CO_2 and exporting inorganic carbon (particulate inorganic carbon) to the ocean floor (Salter et al., 2014; Manno et al., 2018). In the Southern Ocean (Scotia Sea), both foraminifera and pteropods have been found to contribute significantly to the seasonal productivity, with pteropods being the major producer of $CaCO_3$ (Manno et al., 2018).

Productivity patterns in the Arctic are strongly dependent on the degree of sea-ice cover, availability of nutrients and light, and surface stratification (Bluhm et al., 2015). The primary production is characterized by a spring phytoplankton bloom occurring between April and July when the sea ice retreats (Sakshaug, 1997; Lee et al., 2015) and a second phytoplankton bloom in late summer (Wassmann et al., 2019). This production represents the major food source for the zooplankton (Sakshaug, 1997) and references therein.

The northern Barents Sea is located in an Arctic region where rising atmospheric and ocean surface temperatures as well as sea-ice loss are occurring at increasing rates (Descamps et al., 2017). The sea-ice loss may increase the direct gas uptake from the atmosphere, which will have unknown effects on the physical, biogeochemical and ecological conditions (Bates and Mathis, 2009). Because the solubility of CO_2 increases in cold water, and the already low saturation states, the polar oceans in general, and the Barents Sea in particular, are expected to be especially vulnerable to ocean acidification (Chierici and Fransson, 2018). Despite the importance of this region, little is known about the distribution of marine calcifiers, their present state of calcification and how they would respond to ocean acidification. This present study aims to estimate the inorganic and organic carbon standing stocks ($\mu g\ m^{-3}$) and export productivity (flux = $mg\ m^{-2}\ day^{-1}$) of planktic foraminifera and shelled pteropods on the northern margin of Barents Sea, north of Svalbard and into the Arctic Ocean deep Nansen Basin. The calcium carbonate reaching the sea floor derived from planktic foraminifera has been determined to be from 32 to 80% of the total global fluxes (Schiebel, 2002). The diversity of foraminifera in the polar regions is low with dominance of *Neogloboquadrina pachyderma, Turborotalita quinqueloba* and *Globigerina bulloides* (Schiebel et al., 2017). Their vertical distribution has recently been suggested to be delimited to the upper 100 m of the water column (Greco et al., 2019; Meilland et al., 2020). A recent study of the inorganic and organic carbon budgets and the organic-inorganic carbon ratio (C_{ORG}/C_{INORG}) along the southern polar zone in the Southwest Indian Ocean, estimated the C_{ORG}/C_{INORG} to be between 0.17 and 0.5 (Meilland et al., 2018). The inorganic contribution from the planktic foraminiferal faunas represented between 67 and 85% of the total carbon budget and indicates that foraminifera can be a major component in the carbon pump of the ocean. The present study represents the first quantification of carbonate contributions from pteropods and foraminifera from this remote and rarely studied northern Barents Sea area and Nansen basin in the Arctic Ocean.

MATERIALS AND METHODS

Study Area

The northern Svalbard margin is influenced by the flow of warm Atlantic Water, which represents the main supplier of heat to the Arctic Ocean (**Figure 1**). It is conveyed to the area and into the Nansen Basin through the Svalbard Branch of the West Spitsbergen Current (Meyer et al., 2017). The Atlantic water north of Svalbard has a major control of the extent

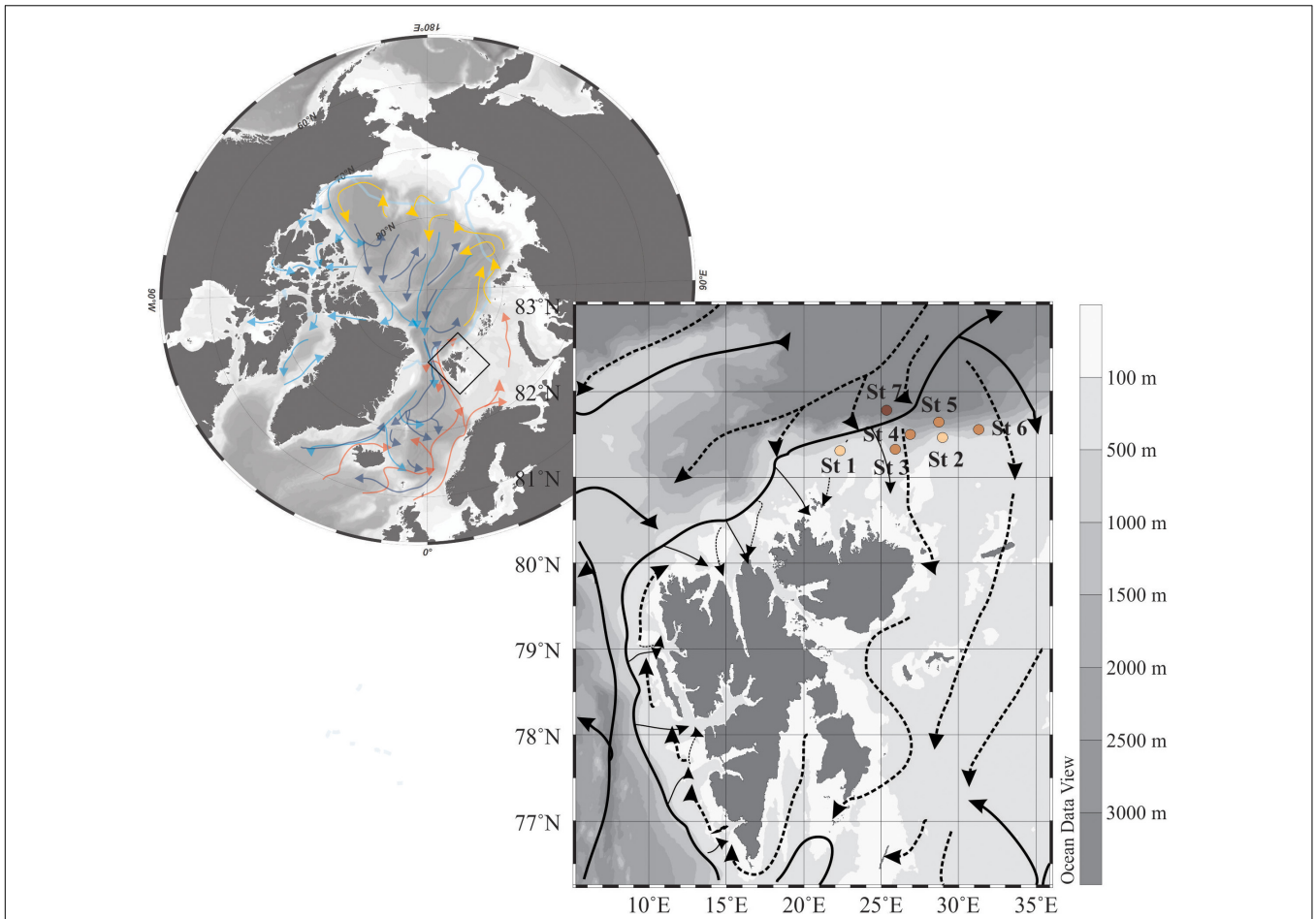

FIGURE 1 | Map of the Arctic Ocean with warm and cold surface, intermediate and deep waters in red, blue, yellow, and dark blue arrows [modified from Anderson and Macdonald (2015). Detailed surface Atlantic (solid line) and Arctic (dashed line) currents from Hop et al. (2019)].Sea ice extent on September 2018 in light blue, and study area framed in black. Zoom in the study area with the sampling stations.

of the sea-ice cover, and has been warming during the last decades (Meyer et al., 2017; Renner et al., 2018) since monitoring started in 1977 (Onarheim et al., 2014). In September 2018, the northern Svalbard margin was ice-free up to 82.40 °N, where the sea-ice edge occurred. This coincided with the fact that 2018 was an anomalously warm year. In September 2018 the Arctic sea-ice cover by area was 25.3% below the 1981–2010 average (NOAA NCFEI, 2018).

Sampling and Sample Analysis

Plankton and water samples were retrieved onboard RV *Helmer Hanssen*, during cruise HH18-6 to the northern Svalbard margin, between August 28 and September 12, 2018. Seven stations were sampled along a longitudinal transect along 81°N, from 22 to 32°E covering the shelf and slope, and the Nansen deep basin in different light conditions (**Figure 1** and **Table 1**). The sampling stations are numbered from west to east: shelf stations

TABLE 1 | Location, latitude (°N) and longitude (°E), water depth (m), sampling date and light conditions, sea surface temperature (°C) and sea surface salinity.

	Location	Latitude (°N)	Longitude (°E)	Water depth (m)	Sampling date	Sampling light conditions	SST (°C)	SSS
St 1	Shelf	81.3	22.3	376	05.09.2018	Night	4.6	34.5
St 2	Shelf	81.5	29.0	368	04.09.2018	Day	4.03	34.4
St 3	Slope	81.3	25.9	510	08.09.2018	Day	3.0	34.0
St 4	Slope	81.5	26.7	1019	04.09.2018	Day	2.8	33.8
St 5	Slope	81.6	28.7	2166	08.09.2018	Night	2.9	34.2
St 6	Slope	81.6	31.3	853	04.09.2018	Night	3.1	34.1
St 7	Basin	81.8	25.3	3094	07.09.2018	Day	1.2	32.9

TABLE 2 | Average size, SD, minimum and maximum value and number of individuals measured.

	Planktic foraminifera				Shelled pteropods			
	>500 μm	250–500 μm	100–250 μm	90–100 μm	>500 μm	250–500 μm	100–250 μm	90–100 μm
Average (μm)		323.3	162.2	95.4	693.1	394.1	226.8	101.7
SD		8.5	46.8	8.7	161.2	70.4	37.0	4.0
Minimum value		309.1	81.5	82.4	438.5	245.8	172.1	97.2
Maximum value		330.3	281. 1	106.6	1371.8	549.6	283.1	104.6
Number of individuals		5	239	13	153	210	14	3

1 and 2, slope stations 3–6, and Nansen Basin deep station 7 (**Figure 1**).

Water Samples

Prior to each plankton tow, the physicochemical parameters of the water column were measured with a CTD (Conductivity, Temperature, Depth) SeaBird 911 Plus equipped with a 12-Niskin bottle Rosette. Seawater for the variables of carbonate chemistry was collected from each Niskin bottle and transferred into 250 mL borosilicate bottles using a silicon tube. The samples were preserved with 50 μL saturated mercuric acid before the post-cruise analyses of dissolved inorganic carbon (DIC) and total alkalinity (AT) at the laboratory of the Institute of Marine Research (IMR), Tromsø, Norway, following standard procedures outlined in Dickson et al. (2007) at a temperature around 25°C. DIC was determined using a coulometric titration with a Versatile Instrument for the Determination of Titration Alkalinity (VINDTA 3D, Marianda, Germany). AT was determined from potentiometric titration with 0.1 N hydrochloric acid in a closed cell using a Versatile Instrument for the Determination of Titration Alkalinity (VINDTA 3S, Marianda, Germany). The accuracy and precision for DIC and AT were assured by repeated measurements of Certified Reference Material (CRM, provided by A. G. Dickson, Scripps Institution of Oceanography, United States), and were ±2 μmol kg^{-1} for both DIC and AT.

Partial pressure of CO_2 (pCO_2), pH and aragonite and calcite saturations (**Ω**) were calculated using DIC and AT in combination with the *in situ* water pressure, salinity, temperature, silicate and phosphate concentrations using the chemical speciation model CO2SYS (Pierrot et al., 2006). The carbonic acid dissociation constants of Mehrbach et al. (1973) as refitted by Dickson and Millero (1987) were used in combination with the bisulfate dissociation constant from Dickson (1990), and the total boron concentration of Lee et al. (2010). The aragonite and calcite stoichiometric solubility constants of Mucci (1983) were used with the pressure corrections of Millero (1979) and the calcium concentration and salinity ratio of Riley and Tongudai (1967).

Planktic Foraminifera and Pteropod Samples

Planktic foraminifera and pteropods were collected using a WP2 zooplankton net (Hydro-bios 90-μm mesh size, Ø = 0.57 m). The upper 300 meters of the water column were towed at regular depth intervals of 0–50 m, 50–100 m, 100–200 m and 200–300 m. The surface layer sample (0–50 m) from station 7 was lost. Immediately after recovery, the samples were frozen at −80°C. The samples were analyzed in the laboratory of the Department of Geosciences, UiT the Arctic University of Norway, Tromsø, Norway.

Each frozen plankton sample was melted and gently wet-sieved with cold water through a cascade of sieves with mesh sizes 500, 250, 100, and 63 μm. Each size fraction obtained (>500, 250–500, 100–250, and 90–100 μm) was wet-picked separately for absolute abundance and flux estimates (note 90 μm was the mesh size of the plankton net) (see below). Only living specimens (containing cytoplasm) of planktic foraminifera and pteropods were counted. Living specimens >100 μm were identified to species level and percentages of individual species calculated. In the following, pteropods >500 μm (most likely young adults) are referred to as large-sized, and size range 250–500 μm (most likely veligers and juveniles) are referred to as medium-sized and, 100–250, and 90–100 μm as small-sized. Planktic foraminifera from the size range 250–500 μm are referred as large-sized, 100–250 μm are referred as medium-sized, and 90–100 μm are referred to as small-sized. The absolute abundance (ind m^{-3}) was calculated dividing the number of individuals by the volume of water sampled with the WP2. The volume was calculated following the general cylinder formula ($V = \pi r^2 h$) where the radius (r) is 0.285 m and h is the height of the target water column depth profile.

In order to estimate the average maximum diameter (Lischka and Riebesell, 2012) of shells per size fraction, 153 (>500 μm), 210 (250–500 μm), 14 (100–250 μm), and 3 (<100 μm) pteropod shells were randomly selected and photographed (**Table 2**) with a DMC4500 camera attached to the binocular Leica Z16 APO (magnification ×0.57–9.2). Their diameter was measured using the software ImageJ (Schneider et al., 2012). We estimated the average dry weight of pteropods (DW) from the average diameter (D) with the equation reported in Bednaršek et al. (2012a) ($DW = 0.137\ D^{1.5005}$). The average individual shell weight was estimated using the calculations described in Bednaršek et al. (2012a). The carbon biomass (μg) of the pteropods was estimated as reported in Bednaršek et al. (2012a) from the dry weight (DW).

In order to estimate the average weight per size fraction, 17 (250–500 μm) and 111 (100–250 μm) foraminiferal shells were

randomly selected, picked and weighed using a Mettler Toledo XP2U (0.1 μg precision) balance.

No treatment to remove the remaining cytoplasm was applied to the shells; therefore the weight acquired also contain organic carbon from the dried cytoplasm, which we consider negligible compared to the shell weight. There is a large density difference between calcite and wet cytoplasm with negligible contribution of the organic carbon to the dry test mass (Schiebel et al., 2007; Beer et al., 2010). The average foraminiferal shell weight was thereafter calculated for each size fraction. In addition, the weight measurements were combined with estimated weights of 5 (250–500 μm), 239 (100–250 μm), and 13 (90–100 μm) foraminiferal shells using the equation reported by Meilland et al. (2018) ($y_m = 2.04 \times 10^{-05} x^{2.2}$) where the mass ($y_w$) is proportional to the minimum diameter (x) of an individual. The average individual weight of calcium carbonate from planktic foraminifera was assumed to be equal to the average individual shell weight. Similarly, the foraminiferal carbon biomass (μg of protein with an estimated 1:1 ratio between protein and organic carbon concentration) was estimated following the equation reported in Meilland et al. (2018) ($y_p = 5.10 \times 10^{-05} x^{1.77}$), where the protein content (y_w) is proportional to the minimum diameter (x) of an individual.

Carbon Standing Stocks and Export Production

The standing stocks (μg m^{-3}) from the upper ocean (0–100 m) were calculated based on the methods described in Meilland et al. (2018). The average weight of $CaCO_3$ (inorganic carbon) and the carbon biomass (organic carbon) of planktic foraminifera and pteropods (μg) were multiplied by integrating the absolute abundance (ind m^{-3}) of the various size fractions from the upper 100 m.

The inorganic carbon production (flux = mg m^{-2} day^{-1}) from foraminifera and pteropods at 100 m (depth of the productive zone) were calculated based on the methods described in Meilland et al. (2018). In this study, the potential inorganic export production at 100 m was derived from the foraminifera and pteropods collected between 50 and 100 m. The depth of 100 m is considered the initial flux level of tests (Schiebel and Hemleben, 2000). The average individual shell weight (μg) or the protein content (μg) (for inorganic and organic carbon, respectively) was multiplied by the absolute abundance of foraminifera and pteropods (ind m^{-3}) and by the test sinking velocity (m day^{-1}) (Schiebel, 2002; Meilland et al., 2018). In case of foraminifera, the test sinking velocity was calculated per size fraction using the formula described by Takahashi and Bé (1984): $Y = 10^a z^b$, where Y is the test sinking velocity (mm s^{-1}), z the shell weight and a and b constants of 2.06 and 0.64, respectively (Schiebel, 2002; Meilland et al., 2018). According to Chang and Yen (2012) the sinking velocity of pteropods is positively correlated with their size, and in this study we used 5 mm s^{-1}. We consider this velocity, even though estimated from a 500-μm shell size, more suitable to apply to all size fractions than other previously reported [e.g., 864–1210 m/day by Lalli and Gilmer (1989)].

RESULTS

Physical and Chemical Environment North of Svalbard

In the study area, the deeper stations (>500 m water depth: slope stations 3, 4, 5 and 6 and basin station 7) are characterized by the presence of Intermediate Water ($-1.1°C < \theta \leq 0°C$), in contrast to the shelf stations 1 and 2 (368–376 m water depth) that are influenced by the Atlantic Water ($\theta > 2.0°C$, $S \geq 34.9$) (Sundfjord et al., 2020; **Figure 2** and **Supplementary Figure 1**). All stations are defined by the presence of a shallow (0–50 m) warm late summer Polar water layer with temperatures of 1–5°C and salinities of 30.17–34.93 (**Figure 2** and **Supplementary Figure 1**). In general, sea surface temperatures from shelf stations not influenced by Arctic deep water are warmer (4–4.6°C) than the slope and basin stations (1.15–3.14°C) (**Table 1**). Moreover, shelf stations have a narrower range of surface salinities (33.68–34.93) compared to deeper stations (30.17–34.55). Specifically, slope station 6 and basin station 7 show a wider range of salinity and the most fresh surface water masses ($S < 30$) are recorded (**Figure 2** and **Supplementary Figure 1**). Beneath this layer, the Atlantic water reaches 500–700 m water depth, with temperature decreasing down to 2°C. The modified Atlantic Water ($0.0°C < \theta \leq 2°C$, $S \geq 34.9$) (Sundfjord et al., 2020) and Intermediate Water are found below the Atlantic water, with temperatures ranging between −0.9 and 1°C and salinity around 34.89 (**Supplementary Figure 1**).

The dissolved inorganic carbon (DIC), total alkalinity (AT) and pCO_2 gradually increase from west to east and from surface to bottom water (**Figure 2**). pH and saturation state α (both aragonite and calcite) generally decrease from surface to bottom (**Figure 2**). The greatest values of DIC (2200 μmol/kg), pH (8.00) and pCO_2 (425 μatm) are recorded below 50 m depth from 29 to 31°E corresponding to the shelf station 2 and slope stations 5 and 6 (**Figure 2**). In these same stations the lowest aragonite (<1.40) and calcite (<2.25) saturation states are recorded in Atlantic Water at 200 m and 150 m depth, respectively. No undersaturated conditions with respect to $CaCO_3$ occur along the transect.

Abundance and Vertical Distribution of Foraminifera and Pteropods

In general, planktic foraminifera dominate in the study area, representing between 68 and 95% of the total community of planktic foraminifera and pteropods together (**Figure 3** and **Table 3**). Planktic foraminifera (<250 μm) are the most abundant and mainly observed between 50 and 300 m (66–95%), whereas the upper 50 m is mainly dominated by pteropods > 250–μm (29–59%) (**Figure 4** and **Supplementary Tables 1,2**). Pteropods are rare or absent below 100 m in any of the stations (**Figures 3–5**).

The planktic foraminiferal fauna along the transect is dominated by *N. pachyderma* and *T. quinqueloba*, followed by *N. incompta* (**Figure 6**). In the entire study area, these three species together represent on average 91.1% of the total assemblage. The lowest occurrence of the three species is 75%

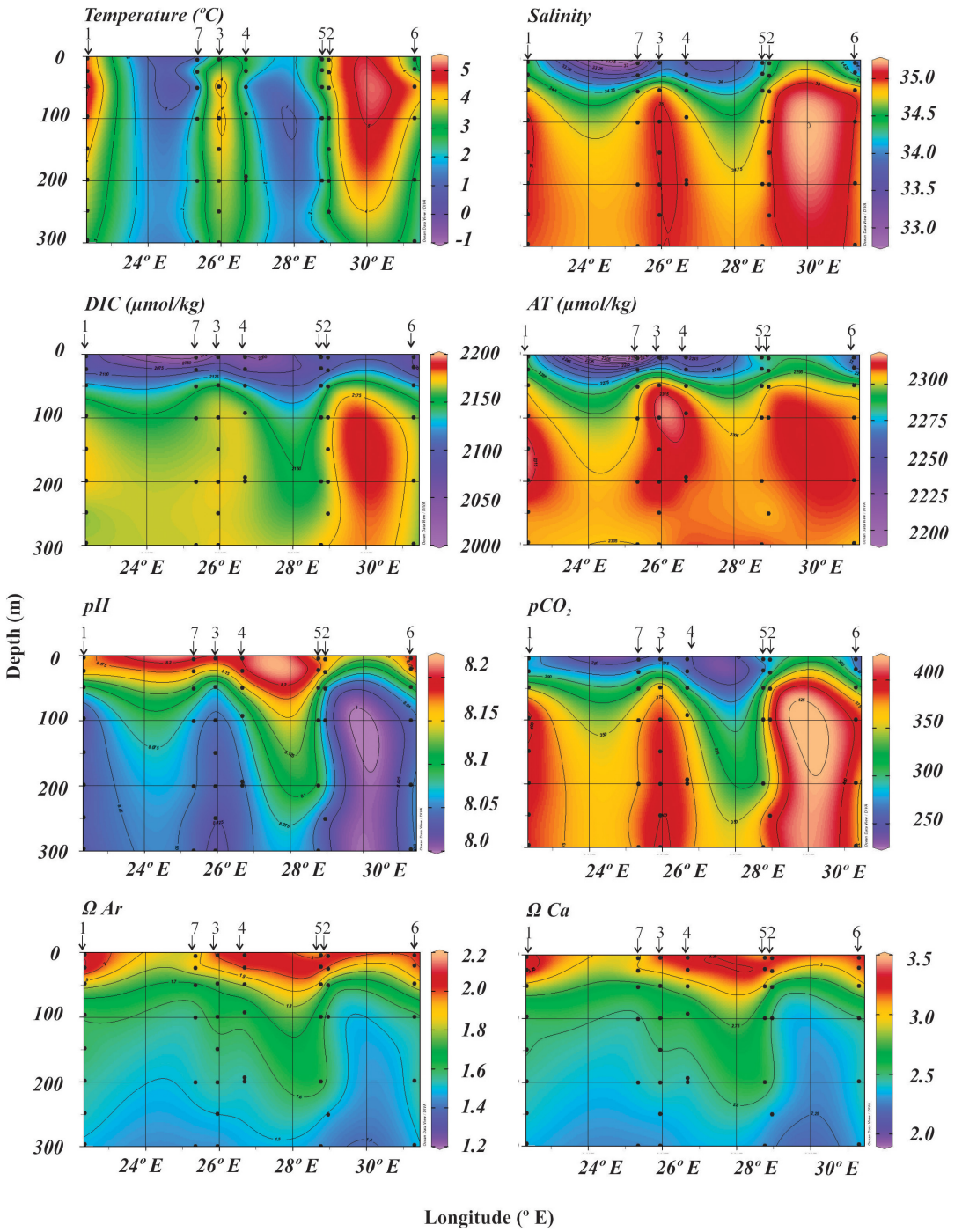

FIGURE 2 | Seawater chemistry sections along the transect. The position of each station represented with black arrows.

(at slope station 6 between 100 and 200 m) and the highest is 100%, in the shallower depth interval of the easternmost shelf station 2 and the north slope station 5 (**Table 4**). The subpolar species *G. bulloides* is part of the foraminiferal community although present in low percentages (**Table 4**). In general, the relative abundance of *N. pachyderma* remains constant in surface samples from all stations in contrast to deeper intervals (**Figure 6**). The highest (73.6% of the total planktic foraminifera community) and the lowest (33.3%) percentages are found at the same depth interval (100–200 m) at stations 4 and 6, respectively (**Table 3**).

The relative abundance of *N. incompta* is variable in the subsurface samples (**Figure 6**). The highest (33.9%) percentages of *N. incompta* is found at 50–100 m at shelf station 1 (**Table 4**).

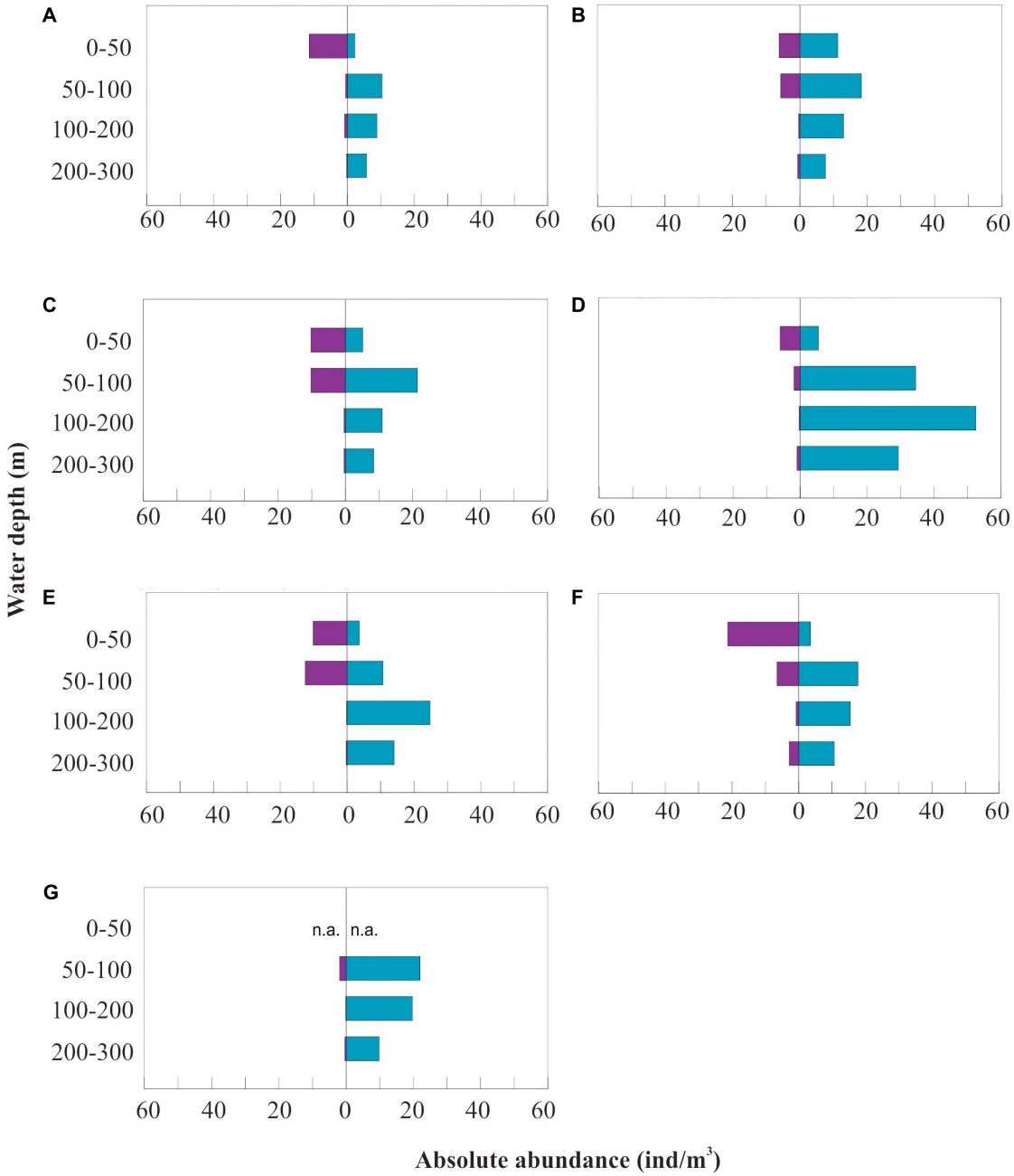

FIGURE 3 | Absolute abundance (ind m^{-3}) of planktic foraminifera (blue) and pteropods (purple) of stations 1–7 **(A–G)** along the water column (n.a., not available).

No specimens are found at the easternmost slope station 6 (**Table 4**).

In general, relatively high percentages of *T. quinqueloba* are found below 50 m water depth with highest relative abundance of 41.2% at slope station 3 and lowest of 8.1% at shelf station 1 and slope station 3 (**Table 3**). The relative abundance of this species below 100 m depth varies between stations (**Figure 6**).

The distribution of *G. bulloides* does not follow any particular pattern and it is generally of low relative abundance (**Table 4**). At slope stations 5 and 6, and basin station 7, the highest percentages of *G. bulloides* are found at 100–200 m depth, while at shelf stations 1 and 2 they occur at 50–100 m depth. At slope stations 3 and 4, the highest abundances are found in the upper 50 m of the water column. This species is most abundant at slope station 3 (12.9%). It is absent at some stations and depths (**Table 4**).

The polar species *Limacina helicina* dominates the pteropod fauna at all stations and depths (94.2–100%). The highest relative abundance of *L. helicina* (100%) was found at shelf station 1, slope stations 3, 4 and 5, and basin station 7 in all sampled intervals. At shelf station 2 and slope station 6 high percentages of *L. helicina*

TABLE 3 | Results of the two-way ANOVA test.

	Foraminifera	Pteropods
	p value	*p* value
Relative abundance/depth	3.2e-06***	2.06e-07***
Relative abundance/size	0.12	0.8
Size/depth	1	1

*Only two size fractions (90–100 and 100–250 μm) were taken into account for foraminifera. ***p < 0.01.*

(>97.2%) occurred in all sampled intervals. Low percentages of *Limacina retroversa* (0.7–5.8%) are found at shelf station 2 (50–100 m) and slope stations 3 (0–100 m) and 6 (0–50 m) (**Table 4**). At slope station 3, which is more influenced by Atlantic Water, is where *L. retroversa* is most abundant (up to 5.8%). No specimens of *L. retroversa* are found below 100 m.

Foraminiferal and Pteropod Carbonate Standing Stock and Export Production in the Upper 100 m of the Water Column

The inorganic standing stocks and export production of foraminifera ranged from 10.6 to 33.1 μg $CaCO_3$ m^{-3}, and from 2.3 to 7.9 mg $CaCO_3$ m^{-2} day^{-1}, respectively. The organic standing stocks and production ranged from 1.9 to 6.2 μg m^{-3}, and from 0.5 to 1.6 mg m^{-2} day^{-1}, respectively. Inorganic standing stocks and export production of pteropods ranged from 57.3 to 439.2 μg $CaCO_3$ m^{-3}, and from 6.1 to 227.6 mg $CaCO_3$ m^{-2} day^{-1}, respectively. The

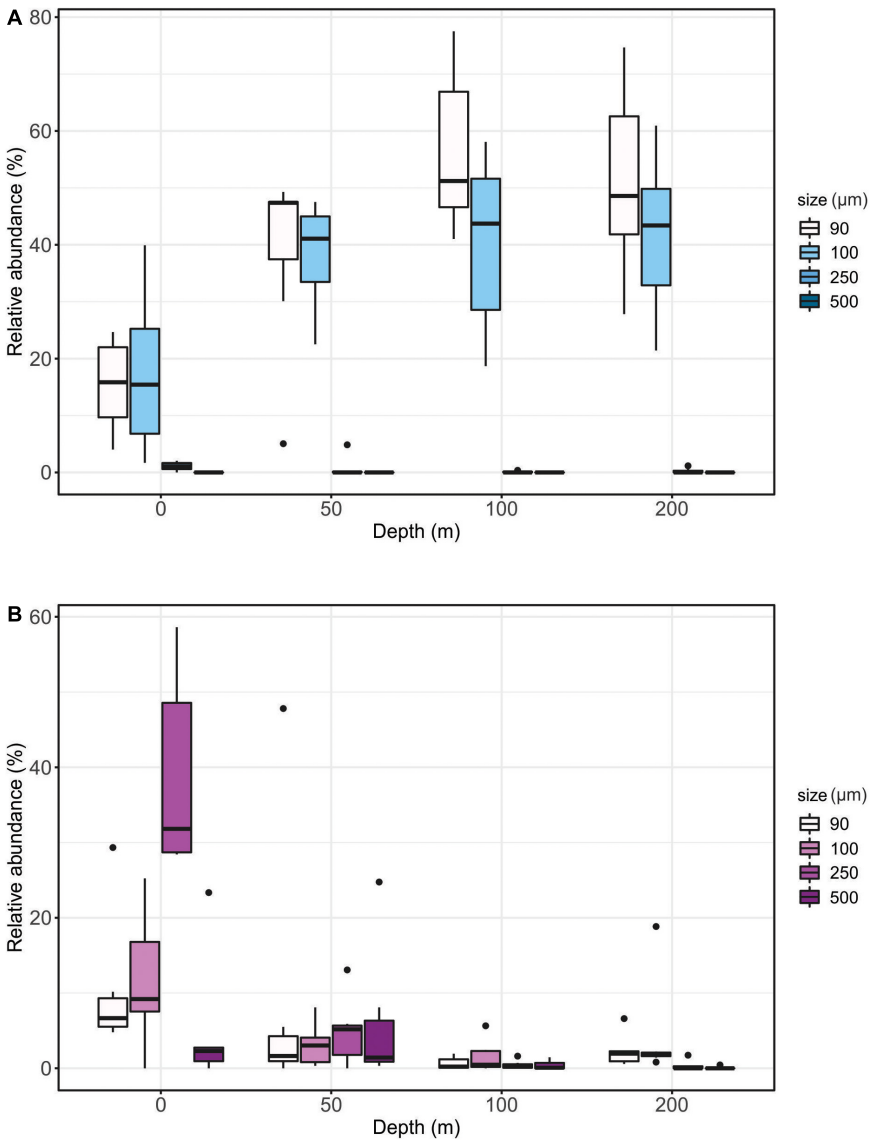

FIGURE 4 | Relative (%) size distribution of planktic foraminifera **(A)** and pteropods **(B)** relative to water depth.

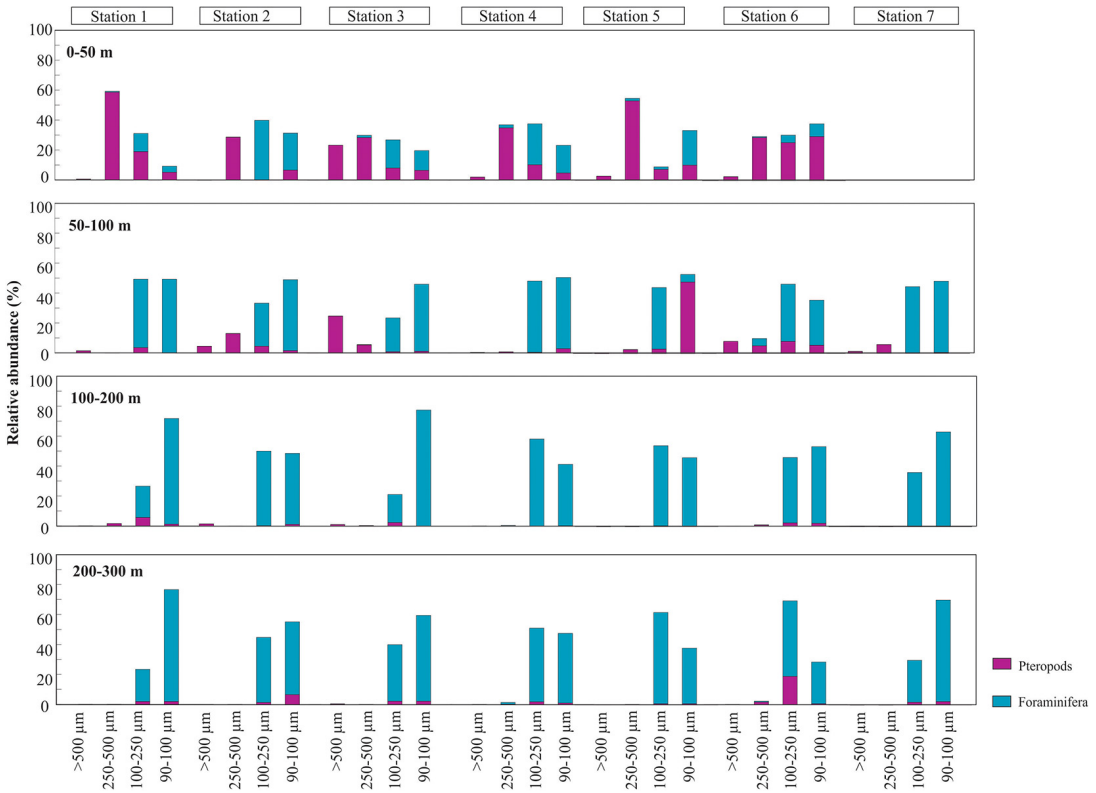

FIGURE 5 | Relative abundance (%) of planktic foraminifera (blue) and pteropods (purple) per size fraction and station. The panels represent from top to bottom: 0 to 50 m, 50 to 100 m, 100 to 200 m, and 200 to 300 m.

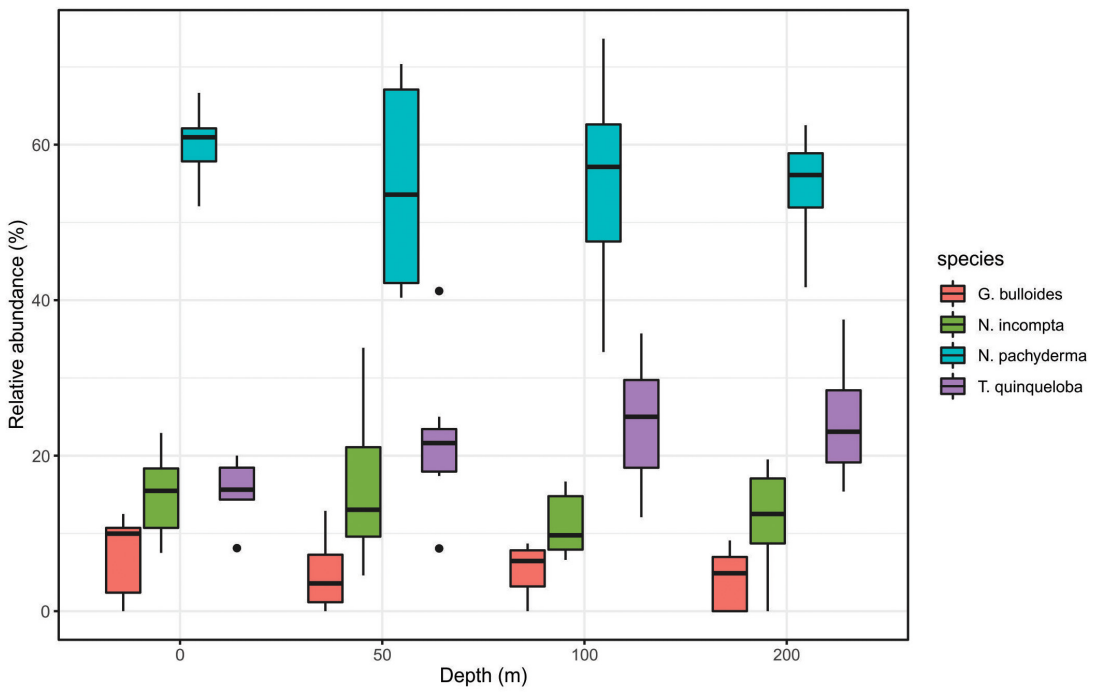

FIGURE 6 | Relative (%) species distribution of planktic foraminifera relative to water depth.

TABLE 4 | Cumulative and absolute abundance (ind m^{-3}) and relative abundance of the main species.

	Cumulative absolute abundance	water depth	Absolute abundance foraminifera	*N. pachyderma*	*T. quinqueloba*	*N. incompta*	*G bulloides*	unknown	Absolute abundance pteropods	*L. helicina*	*L. retroversa*
ST 1	10.09	0–50	**2.3**	61.9	19.0	9.5	9.5	0.0	**11.4**	100	0.00
		50–100	**10.4**	40.3	8.1	33.9	12.9	4.8	**0.6**	100	0.00
		100–200	**8.9**	43.5	30.4	8.7	8.7	8.7	**0.8**	100	0.00
		200–300	**5.8**	53.8	23.1	15.4	0.0	7.7	**0.2**	100	0.00
ST 2	15.79	0–50	**11.3**	57.1	14.3	14.3	0.0	14.3	**6.2**	100	0.00
		50–100	**18.3**	70.4	18.5	7.4	3.7	0.0	**5.7**	97.26	2.74
		100–200	**13.0**	57.1	35.7	7.1	0.0	0.0	**0.4**	100	0.00
		200–300	**7.6**	62.5	25.0	12.5	0.0	0.0	**0.7**	100	0.00
ST 3	16.81	0–50	**5.2**	62.2	8.1	18.9	10.8	0.0	**10.3**	94.17	5.83
		50–100	**21.4**	41.2	41.2	11.8	0.0	5.9	**10.3**	97.69	2.31
		100–200	**10.9**	66.7	12.5	16.7	4.2	0.0	**0.4**	100	0.00
		200–300	**8.4**	41.7	37.5	8.3	0.0	12.5	**0.4**	100	0.00
ST 4	32.72	0–50	**5.5**	52.1	14.6	22.9	10.4	0.0	**6.0**	100	0.00
		50–100	**34.5**	69.0	21.8	4.6	2.3	2.3	**1.8**	100	0.00
		100–200	**52.6**	73.6	12.1	6.6	2.2	5.5	**0.3**	100	0.00
		200–300	**29.4**	50.0	31.8	9.1	9.1	0.0	**0.9**	100	0.00
ST 5	19.11	0–50	**3.7**	66.7	16.7	16.7	0.0	0.0	**10.2**	100	0.00
		50–100	**10.7**	43.2	21.6	24.3	10.8	0.0	**12.5**	100	0.00
		100–200	**24.8**	51.6	29.0	12.9	6.5	0.0	**0.2**	100	0.00
		200–300	**14.1**	56.1	19.5	19.5	4.9	0.0	**0.3**	100	0.00
ST 6	19.70	0–50	**3.5**	60.0	20.0	7.5	12.5	0.0	**21.3**	99.29	0.71
		50–100	**17.7**	65.2	17.4	13.0	0.0	4.3	**6.5**	100	0.00
		100–200	**15.4**	33.3	25.0	16.7	8.3	16.7	**0.8**	100	0.00
		200–300	**10.7**	61.5	15.4	0.0	7.7	15.4	**2.9**	100	0.00
ST 7	17.99	0–50									
		50–100	**22.0**	53.6	25.0	17.9	3.6	0.0	**2.0**	100	0.00
		100–200	**19.7**	58.5	24.4	9.8	7.3	0.0	**0.1**	100	0.00
		200–300	**9.8**	56.3	18.8	18.8	6.3	0.0	**0.4**	100	0.00

The bold was used to differenciate the total absolute abundance to the species relative abundance.

organic standing stocks and production ranged from 18.6 to 142.5 μg m^{-3}, and from 2.0 to 73.9 mg m^{-2} day^{-1}.

Shelf

On the shelf, the absolute abundance of planktic foraminifera and pteropods increases from west (station 1, 12.3 ind m^{-3} from 0–100 m and 11 ind m^{-3} from 50–100 m) to east (station 2, 20.7 ind m^{-3} from 0–100 m and 24 ind m^{-3} from 50–100 m) (**Figure 3** and **Tables 5**, **6**).

The westernmost station 1 is where we find the lowest abundance of planktic foraminifera of all the stations in the transect (6.4 ind m^{-3} and 10.4 ind m^{-3}, from 0–100 m and 50–100 m, respectively) (**Figure 3** and **Tables 5**, **6**). Thus, we estimate the lowest foraminiferal inorganic (10.6 μg $CaCO_3$ m^{-3}) and organic (1.9 μg m^{-3}) carbon standing stocks and inorganic (2.3 mg m^{-2} day^{-1}) and organic (0.5 mg m^{-2} day^{-1}) export production (**Tables 5**, **6**). Moreover, the lowest pteropod production (6.1 mg $CaCO_3$ m^{-2} day^{-1} and 2.0 mg m^{-2} day^{-1} of organic carbon) is estimated at this westernmost shelf station causing the lowest inorganic carbon (8.4 mg m^{-2} day^{-1}) and carbon (2.4 mg m^{-2} day^{-1}) export production in our transect (**Table 6**).

Slope

Over the slope, the integrated abundances of planktic foraminifera and pteropods in the upper 100 m are highest at stations 3, 4 and 6 (23.6–24.5 ind m^{-3}) (**Figure 3** and **Table 5**). The vertically integrated abundance of planktic foraminifera is highest at the westernmost station 4 (20 ind m^{-3}) while pteropods, increase from west (station 4, 3.9 ind m^{-3}) to east (station 6, 13.9 ind m^{-3}) (**Figure 3** and **Table 5**).

At the same time, the abundances of planktic foraminifera and pteropods at the subsurface (50–100 m) decrease from west (stations 3 and 4, 31.7 ind m^{-3} and 36.3 ind m^{-3}) to east (stations 5 and 6, 23.3 ind m^{-3} and 24.2 ind m^{-3}) (**Figure 3** and **Table 6**). The highest inorganic (459.5 μg $CaCO_3$ m^{-3}) and organic (146.2 μg m^{-3}) standing stocks and inorganic (231.3 mg $CaCO_3$ m^{-2} day^{-1}) and organic (74.6 mg m^{-2} day^{-1}) export production are found at slope station 3 (**Tables 5**, **6**).

TABLE 5 | Integrated (upper 100 m) absolute abundance (m^{-3}) and derived $CaCO_3$ standing stocks ($\mu g\ m^{-3}$) and carbon biomass ($\mu g\ m^{-3}$) and the contribution from planktic foraminifera and pteropods.

	Integrated abundance (m^{-3})	$CaCO_3$ ($\mu g\ m^{-3}$)	Carbon biomass ($\mu g\ m^{-3}$)	Foraminifera abundance (m^{-3})	Foraminifera $CaCO_3$ ($\mu g\ m^{-3}$)	Foraminifera C biomass ($\mu g\ m^{-3}$)	Pteropod abundance (m^{-3})	Pteropod $CaCO_3$ ($\mu g\ m^{-3}$)	Pteropod C biomass ($\mu g\ m^{-3}$)
Station 1	12.3	140.1	44.0	6.4	10.6	1.9	6.0	129.5	42.0
Station 2	20.7	171.6	52.3	14.8	23.2	4.2	6.0	148.4	48.1
Station 3	23.6	459.5	146.2	13.3	20.3	3.6	10.3	439.2	142.5
Station 4	23.9	111.8	31.5	20.0	33.1	6.0	3.9	78.7	25.6
Station 5	18.6	161.6	50.5	7.2	13.8	2.6	11.4	147.8	48.0
Station 6	24.5	269.1	84.5	10.6	20.8	3.9	13.9	248.3	80.6
Station 7*	23.9	86.4	24.8	22.0	29.2	6.2	2.0	57.3	18.6

**The surface sample of the Nansen Basin station 7 was missing, therefore the values presented here are considering only the subsurface samples.*

TABLE 6 | Absolute abundance (m^{-3}) from 50 to 100 m and derived $CaCO_3$ export production ($mg\ m^{-2}\ d^{-1}$) and carbon biomass ($mg\ m^{-2}\ d^{-1}$) and the contribution from planktic foraminifera and pteropods.

	Abundance (m^{-3})	$CaCO_3$ ($mg\ m^{-2}\ d^{-1}$)	Carbon biomass ($mg\ m^{-2}d^{-1}$)	Foraminifera abundance (m^{-3})	Foraminifera $CaCO_3$ ($mg\ m^{-2}\ d^{-1}$)	Foraminifera C biomass ($mg\ m^{-2}d^{-1}$)	Pteropod abundance (m^{-3})	Pteropod $CaCO_3$ ($mg\ m^{-2}\ d^{-1}$)	Pteropod C biomass ($mg\ m^{-2}\ d^{-1}$)
Station 1	11.0	8.4	2.4	10.4	2.3	0.5	0.6	6.1	2.0
Station 2	24.0	73.4	23.4	18.3	3.3	0.7	5.7	70.1	22.8
Station 3	31.7	231.3	74.6	21.4	3.7	0.7	10.3	227.6	73.9
Station 4	36.3	18.1	4.9	34.5	7.9	1.6	1.8	10.3	3.3
Station 5	23.3	31.5	9.7	10.7	4.1	0.8	12.5	27.4	8.9
Station 6	24.2	84.3	26.1	17.7	7.2	1.1	6.5	77.1	25.0
Station 7	23.9	29.6	9.0	22.0	4.9	1.0	2.0	24.7	8.0

Basin

In the basin station the surface sample was missing, therefore we only have subsurface data (50–100 m) to estimate the standing stocks and production. This station shows high concentration of planktic foraminifera (22 ind m^{-3}) and a negligible concentration of pteropods (2 ind m^{-3}) (**Figure 3** and **Table 4**). We estimate here the lowest total inorganic (86 $\mu g\ m^{-3}$) and organic (24.8 $\mu g\ m^{-3}$) carbon standing stock in our transect and a relatively low inorganic (29.6 $mg\ m^{-2}\ day^{-1}$) and organic (9 $mg\ m^{-2}\ day^{-1}$) carbon export production (**Tables 5**, **6**).

DISCUSSION

Vertical Distribution

In this particular area and time of the year, the absolute abundance of planktic foraminifera is higher below 50 m depth correlating in high salinity water ($\approx$ 35), while pteropods are more abundant at the surface, when salinity is lower than 34.5 (**Table 3**, **Figures 3–5**, and **Supplementary Tables 1**, **2**). There is no clear correlation between the distribution of planktic foraminiferal abundance and depth in the water column ($R = 0.11$), while it correlates well with the carbonate chemistry in the water column of total alkalinity ($p < 0.01$), DIC ($0.05 > p > 0.01$), Ω_{CA} ($0.1 > p > 0.05$), salinity ($0.1 > p > 0.05$), and water mass density ($0.05 > p > 0.01$) (**Table 7**). The distribution of pteropods is significantly correlated ($p < 0.01$) to depth in the water column, and all parameters from the carbonate water chemistry (AT, DIC, pH, pCO_2 and Ω_{AR}), salinity and water mass density (**Table 7**). This close correlation between pH or Ω_{AR}, and the distribution of pteropods (low abundance of pteropods correlate with low values of pH and Ω_{AR}) (**Table 7**) could possibly be a cause of effects of ocean acidification. However, since carbonate chemistry also correlate strongly with depth ($p < 0.01$) this is probably a causal relationship (one variable having a direct influence on another variable). Further studies on a seasonal basis covering at least one year are thus needed to understand the eventual effects of ocean acidification in the area.

The distribution of foraminiferal specimens among the different size fractions does not vary between the different depth intervals on a statistically significant basis (**Figure 4**). It is important to stress that this might be biased by the wide size fractions we are working with (most of the populations belongs to the size fractions between 90–250 μm) and by the very low numbers of foraminifera systematically found in the size classes $>250\ \mu m$. As previously reported from the Arctic region, almost no foraminifera has been found in the 250–500 μm size fraction and none $>500\ \mu m$ (Carstens and Wefer, 1992; Carstens et al., 1997) similar to our study.

As also reported for the central Barents Sea and eastern Fram Strait (Carstens et al., 1997; Manno and Pavlov, 2014; Pados and Spielhagen, 2014; Ofstad et al., 2020), the highest concentration of planktic foraminifera occurs between 50–100 m

TABLE 7 | Correlation table between environmental parameters, carbonate chemistry and distribution of planktic foraminifera and pteropods.

	depth	AT	DIC	pH	pCO2	Ω_{CA}	Ω_{AR}	Salinity	Temperature	Density
AT	0.53***									
DIC	0.69***	0.94***								
pH	−0.72***	−0.83***	−0.95***							
pCO2	0.65***	0.83***	0.93***	−0.99***						
Ω_{CA}	−0.83***	−0.73***	−0.92***	0.92***	−0.88***					
Ω_{AR}	−0.83***	−0.72***	−0.91***	0.91***	−0.87***	1***				
Salinity	0.65***	0.96***	0.96***	−0.93***	0.93***	−0.82***	−0.81***			
Temperature	−0.18	0.23	0.08	−0.23	0.31	0.16	0.17	0.29		
Density	0.74***	0.92***	0.98***	−0.9***	0.86***	−0.91***	−0.91***	0.95***	−0.03	
Foraminifera	0.11	0.5***	0.43**	−0.32	0.3	−0.37*	−0.37**	0.37*	−0.28	0.46**
Pteropods	−0.66***	−0.61***	−0.69***	0.64***	−0.6***	0.73***	0.73***	−0.65***	0.3	−0.74***

*$0.1 > p > 0.05$; **$0.05 > p > 0.01$; ***$p < 0.01$.

and 100–200 m water depth correlating with water masses of Atlantic origin (**Figure 3**). At the same time, the abundance range presented here (7–34 ind m^{-3}) agrees well with previous results reporting between 3 and 29 ind m^{-3} in the early summer at the Fram Strait (Pados and Spielhagen, 2014). However, the abundances presented in our study are generally lower than previously reported abundances from the central Barents Sea for early summer (12–436 ind m^{-3}) (Ofstad et al., 2020) and in the western Barents Sea for late summer (0–400 ind m^{-3}) (Meilland et al., 2020). The discrepancy could be caused by seasonality and/or differences in environmental conditions (higher sea surface temperature and higher surface salinity) and regime (Atlantic), confirmed by dominance of Atlantic or sub-polar species (mainly *T. quinqueloba*) in these more southerly locations than in our study area in the north. In addition, the stations in the central Barents Sea are affected by methane seepage, which may have contributed to the higher concentrations and productivity (Ofstad et al., 2020). Methane seepage have been considered as areas of increased primary productivity [Ofstad et al. (2020) and referenced therein]. However, in both the central Barents Sea and northern Svalbard margin, planktic foraminifera show similar vertical distribution patterns in the water column. Considering the differences in sampling time (day/night), foraminiferal distribution in the study area seems to not be affected by diurnal vertical migration [as also reported by Ofstad et al. (2020)] and as reported from the subtropical North Atlantic (Meilland et al., 2020). This agrees with previous studies reporting no evidence of diel vertical migration in the Fram Strait of *N. pachyderma* and *T. quinqueloba* during the midnight-sun season (Manno and Pavlov, 2014) and in the Arctic and North Atlantic of *N. pachyderma* (Greco et al., 2019).

Medium-sized pteropods (>250 μm) dominate the upper 100 meters of the water column and are scarcely present at depth below 200 m (**Figures 4**, **5**). The absolute abundance of pteropods is generally higher between 0 and 50 m water depth in summer in the central Barents Sea, as previously reported by Ofstad et al. (2020). This pattern is also observed in other polar regions (Indian sector of the Antarctic Ocean) where over 90% of *L. helicina* were found in the upper 100 m of the water column (Akiha et al., 2017). Pteropods are concentrated in the upper water column at night [Fabry (1989) and references therein]. Specifically in the Arctic, patterns of diurnal vertical migrations of the pteropod *L. helicina* have been observed during autumn (Falk-Petersen et al., 2008). Adults of *L. helicina* are able to descend to deep waters during the day and ascend to the surface during the night to avoid predation, mainly from cods (Falk-Petersen et al., 2008). However, the negligible concentrations (average < 15% of the total assemblage) found in our study below 100 m do not follow any particular pattern regarding the presence or absence of light and the sampling time.

Species Distribution – Relative Abundance

In summer in the Fram Strait, Pados and Spielhagen (2014) attributed the distribution of the polar species *N. pachyderma* to polar water masses [characterized by lower temperature, pH and $CaCO_3$ saturation (Shadwick et al., 2013)] and the sub-polar species *T. quinqueloba*, to the Atlantic water masses (characterized by higher pH and $CaCO_3$ saturation). The polar species *N. pachyderma* thus might be more resistant and/or better adapted to waters with lower pH and $CaCO_3$ saturation than the subpolar species *N. incompta*, *T. quinqueloba* and *G. bulloides*. The highest integrated vertical concentration of planktic foraminifera and pteropods (32.72 ind m^{-3}) (from 0 to 300 m depth) is found at slope station 4 (**Table 4**). This station is crossed by the Atlantic current which brings warm and nutrient rich waters to the Arctic Ocean and an influx of various planktic organisms [Hop et al. (2019) and references therein] (**Figure 1**). This station is also characterized by a high surface pH (8.2) and a relatively high Ω_{CA} and Ω_{AR} typical for the Atlantic water mass (**Figure 2**). The integrated upper 300 m concentration from this station is caused by the high concentrations of planktic foraminifera and pteropods found between 100 and 200 m (**Figure 3**). This depth range, characterized by relatively cold Atlantic Water (2°C), is dominated by foraminifera in the size fractions between 90–250 μm (**Figure 5**). The dominant species are *N. pachyderma* and *N. incompta*. The presence of other warmer water species such as *T. quinqueloba* and *G. bulloides* (**Table 4**) might be indicative of a highly productive

environment and high food availability (Volkmann, 2000). The lowest integrated vertical concentrations of foraminifera and pteropods (10.09 ind m^{-3}) are found at shelf station 1, the westernmost station. The station, which also records the lowest abundances at each depth, is dominated by small specimens (90–100 μm) of *N. pachyderma*. The low abundances of warmer water species recorded at this station from surface to 300 m, which are the lowest found in the whole transect, might be indicative of low productivity and food availability and no input from warmer waters, which in general correlate with low concentrations of marine calcifiers.

The high proportion of both the polar species *N. pachyderma* and the subpolar species *T. quinqueloba* at the northern Svalbard margin agrees well with results reported in previous studies from the Fram Strait (Carstens et al., 1997; Volkmann, 2000; Husum and Hald, 2012; Manno and Pavlov, 2014; Pados and Spielhagen, 2014) and Nansen Basin (Carstens and Wefer, 1992). However, studies in the Arctic Ocean from plankton tows and sediment reconstructions from the Holocene reported a monospecific faunal assemblage consisting of *N. pachyderma* [Bauch (1999) and references therein]. In our study the highest relative abundance of *N. pachyderma* usually occurs in the upper 100 m of the water column. The distribution observed here agrees with a previous study at high northern latitudes reporting that *N. pachyderma* is found all along the upper water column, but being most abundant in the subsurface below 50 m (Greco et al., 2019). Thus, *N. pachyderma* does not behave as a deep-dweller species [as reported for high latitudes by Kohfeld et al. (1996) and references therein] and as previously observed in the Sea of Okhotsk (Bauch et al., 2002). The depth of calcification of this species has been reported to be between 25 to 70 m in the western part of the Fram Strait (Simstich et al., 2003). The depth of calcification is thought to be related to their optimum habitat and environmental conditions [Weinkauf et al. (2016) and references therein]. The relative abundance of *N. pachyderma* presented here (average: 55.9%; range 33–74%) is lower than the percentages reported recently in the Fram Strait (76–90%) (Pados and Spielhagen, 2014). Here, the highest percentages (90%) of *N. pachyderma* were found at sea-ice covered stations, where a higher absolute abundance was found as well (Pados and Spielhagen, 2014). Thus, we can possibly attribute our lower values to the absence of sea ice in our sampling area. The highest relative abundance of *T. quinqueloba* is found between 100 and 200 m below the surface (**Figure 6**). In the Barents Sea in general, it prefers the deeper waters between 100 and 200 m and areas influenced by relatively warm Atlantic waters (Volkmann, 2000). This species dominates (>80%) the faunal composition in the south-western Svalbard margin, followed by *N. pachyderma* (>10%) and *G. uvula* and *N. incompta* (<5%) (Zamelczyk et al., 2020). The relative abundance of *T. quinqueloba* found in this transect (average: 21.7%; range 8–41%) surpass previous values reported from the Fram Strait (5–23%) (Pados and Spielhagen, 2014). As suggested by the authors, the maximum productivity of this species is expected to occur in early autumn (Pados and Spielhagen, 2014), which was the time when our samples were collected.

The relative abundance of *N. incompta* observed in our samples (average: 13.5%; range 7–34%) exceeds the values that have been published before. In the Fram Strait, Pados and Spielhagen (2014) reported that this species contributed, together with *G. bulloides*, less than 9% of the total assemblage. Also, a recent study observed an average percentage of *N. incompta* of 1% in June 2016 along a transect in the central Barents Sea (Ofstad et al., 2020). In the central Barents Sea, the relative abundances of subarctic species such as *N. incompta*, are increasing compared to preindustrial records (Jonkers et al., 2019; Meilland et al., 2020; Ofstad et al., 2020). The higher relative abundances observed can be a result of the so-called 'Atlantification.' This process is caused by an increasing influence (both in volume and heat) of warm Atlantic water inflow (Årthun et al., 2012). Moreover, the seasonal difference might be a factor affecting the relative abundances of this species, where the June samples in the central Barents Sea [Ofstad et al. (2020) would be recording spring characteristics], whereas September, represents late summer or early fall. In addition, the northern Svalbard margin could be more affected by the Atlantic inflow and to the 'Atlantification' processes than the central Barents Sea. A previous study conducted in the same area north of Svalbard has reported the presence of tropical adiolarian associated with an episode of strong and warm Atlantic inflow (Bjørklund et al., 2012).

Earlier studies of planktic foraminiferal faunas collected by plankton tows in the Arctic Ocean have reported absence of *G. bulloides* (Volkmann, 2000). However, it has been suggested that this species can be transported sporadically to the Arctic Ocean by the Atlantic water masses (Volkmann, 2000). In our study, we attribute the presence and relatively high concentrations of living *G. bulloides* (average: 5.2%; range < 12.9%) and of *N. incompta*, to an 'Atlantification' process.

It is noteworthy that we only considered living specimens (containing cytoplasm) of planktic foraminifera and pteropods, thus our results suggest that certain subpolar planktic foraminferal and pteropod species can survive in this high-Arctic environment, probably as long as 'Atlantic' conditions prevail.

A recent study by Kacprzak et al. (2017) have reported pteropod abundances from both Arctic and Atlantic water masses in the Nordic Seas. They found absolute abundances of *L. helicina* ranging from 0.056 to 12 ind m^{-3} and *L. retroversa* from 0.002 to 52 ind m^{-3}. The highest abundance of *L. helicina*, which is comparable to our results (1.6–5.9 ind m^{-3}), were found in Arctic water (Kacprzak et al., 2017). The high abundance of *L. retroversa* reported by Kacprzak et al. (2017) is indicative of an Atlantic-influenced environment. The presence of the subpolar pteropod *L. retroversa* at slope stations 3, 4 and 6 could be interpreted as a stronger influence of the warmer Atlantic waters on the northern Svalbard margin. An increase in the Atlantic water inflow was observed in this area between summer and late fall of 2018 (Kolås et al., 2020).

Biogenic Carbonate Standing Stocks and Export Production

The organic-inorganic carbon ratio (C_{ORG}/C_{INORG}) from planktic foraminifera and pteropods is estimated to be between

0.28 and 0.32 (**Tables 8**, **9**). Thus, the inorganic carbon from planktic foraminifera and pteropods represents between 76 and 79% of the total carbon they generate (relative to the sum of estimated organic and inorganic carbon) (**Tables 8**, **9**). The inorganic contribution (76%) of pteropods is lower than the foraminiferal contribution (82−87%) (**Tables 8**, **9**). This agrees well with results from other polar regions where foraminiferal inorganic carbon represents between 67 and 85% of the total carbon (Meilland et al., 2018). Hence, we focus the discussion on the inorganic standing stocks and export production from the planktic foraminifera and pteropods.

Despite the higher absolute abundances of planktic foraminifera in the upper 100 m of the water column (**Figures 3**, **5**), pteropods contribute 66–96% to the inorganic carbon standing stocks compared to 4–34% by the planktic foraminifera (**Table 8**). This suggests that the estimates of inorganic carbon standing stocks largely depends on the size of the organisms. In this study, the foraminiferal test size is smaller than pteropods from the same size fraction on average (**Table 2**). Moreover, negligible abundances of planktic foraminifera are found in the larger size fractions, with few individuals in the size fraction 250–500 μm and none >500 μm (**Figure 5**). The inorganic carbon standing stocks and flux (export production) reported in the present study are derived from living individuals; hence there could be an underestimation. Considering empty shells of dead individuals could lead to larger standing stocks and production values.

The highest inorganic carbon standing stocks in the upper 100 m of the water column (shelf station 2 and slope stations 3 and 6) are the stations where large pteropods (>500 μm) show high abundances (0.6–5.7 ind m^{-3}) (**Table 8** and **Figure 5**). In these stations we also find the subpolar species *L. retroversa* (**Table 4**) and the highest influence of Atlantic Water. The lowest inorganic carbon standing stock (basin station 7) is where the contribution of pteropods is the lowest (66.6%) (**Table 8**). This station is only represented by the subsurface samples (due to loss of the surface sample 0–50 m), therefore this value is most probably an underestimation.

The highest standing stocks of foraminifera are found at slope station 4 and basin station 7 (**Table 8**), where the lowest surface temperatures and salinities are found (2.76°C and 33.77; 1.15°C and 32.94, respectively). However, the values from station 7 could be overestimated because of the loss of the surface sample 0–50 m. The highest standing stocks from pteropods are found at the slope station 3, with relatively cold and fresh surface waters (T < 3° C and S < 34). The lowest standing stocks from pteropods are found at the slope station 4 and basin station 7, which are strongly influenced by low surface salinity from melting sea ice (33.77 and 32.94, respectively). However, the lower standing stocks from pteropods found at station 7 could be an underestimation. As previously discussed, in general pteropods are more abundant from 0 to 50 m depth and this sample is missing.

The absolute abundances found between 50 and 100 m depth are mainly from planktic foraminifera (38.8–91.8%), rather than pteropods (8.2–61.2%). Even though the inorganic carbon flux estimates come from those abundances, pteropods contribute significantly more (56.7–98.4%) to the total inorganic carbon export production than the planktic foraminifera (1.6–43.4%)

TABLE 8 | Total, and foraminiferal and pteropod organic:inorganic carbon ratio, foraminifera and pteropod inorganic contribution to the total carbon and foraminifera and pteropod inorganic contribution to the total inorganic standing stocks.

	Total OC:IC	Foraminifera OC:IC	Foraminifera IC/TC (%)	Pteropod OC:IC	Pteropod IC/TC (%)	Foraminifera/total CaCO3 (%)	Pteropod/total CaCO3 (%)
Station 1	0.3	0.2	84.8	0.3	75.5	7.6	92.4
Station 2	0.3	0.2	84.7	0.3	75.5	13.5	86.5
Station 3	0.3	0.2	84.9	0.3	75.5	4.4	95.6
Station 4	0.3	0.2	84.7	0.3	75.5	29.6	70.4
Station 5	0.3	0.2	84.1	0.3	75.5	8.5	91.5
Station 6	0.3	0.2	84.2	0.3	75.5	7.7	92.3
Station 7*	0.3	0.2	82.5	0.3	75.5	33.8	66.3

**The surface sample of the Nansen Basin station 7 was missing, therefore the values presented here are considering only the subsurface samples.*

TABLE 9 | Total, and foraminiferal and pteropod organic:inorganic carbon ratio, foraminifera and pteropod inorganic contribution to the total carbon and foraminifera and pteropod inorganic contribution to the total inorganic export production.

	Total OC:IC	Foraminifera OC:IC	Foraminifera IC/TC (%)	Pteropod OC:IC	Pteropod IC/TC (%)	Foraminifera/total CaCO3 (%)	Pteropod/total CaCO3 (%)
Station 1	0.3	0.2	82.1	0.3	75.3	27.4	72.6
Station 2	0.3	0.2	82.5	0.3	75.5	4.5	95.5
Station 3	0.3	0.2	84.1	0.3	75.5	1.6	98.4
Station 4	0.3	0.2	83.2	0.3	75.7	43.6	56.9
Station 5	0.3	0.2	83.7	0.3	75.5	13.0	87.0
Station 6	0.3	0.2	86.7	0.3	75.5	8.5	91.5
Station 7	0.3	0.2	83.1	0.3	75.5	16.6	83.4

(**Table 9**). The high contribution of pteropods agrees with a previous study reporting that pteropods represents between 60 and 100% of the vertical productivity of calcium carbonate in autumn in the Lofoten Basin in the Norwegian Sea (Drits et al., 2020), and between 55 and 83% in the northern Scotia Sea (Manno et al., 2018). The highest inorganic carbon export production (slope stations 3 and 6 and shelf station 2) are the stations where pteropods contribute the most (91–98%), whereas the lowest (shelf station 1 and slope station 4), they contribute 56–72% (**Table 9**). The highest inorganic carbon flux at slope station 3 is caused by a relatively high abundance (7.8 ind m^{-3}) of pteropods >500 μm between 50 and 100 m compared to the other stations (0.008–1.96 ind m^{-3}). Even though the highest inorganic carbon standing stocks and flux are found at the same stations, they are not directly proportional to one another (**Tables 5**, **6**). This is particularly true for shelf station 2 and slope station 6. The differences between the standing stocks and the flux at stations 2 and 6 are caused by the greater abundances of large specimens in the size fraction 250–500 μm at station 6 compared to station 2, which is dominated by individuals <100 μm.

Only few studies have reported the contribution of planktic foraminifera and pteropods to the inorganic carbon budgets and production from plankton tows (Bednaršek et al., 2012a; Buitenhuis et al., 2013). In these studies, there are no agreement about the mesh-size used (100, 150, 180, 200, 300, and 333 μm) or the sampling depth (upper 200, upper 300 m or to the bottom), which influences the size and abundance of organisms captured by the nets (Bednaršek et al., 2012a). In any of these studies, authors combine data of planktic foraminifera and shelled pteropods in the northern Svalbard margin. Thus, in order to be able to compare the standing stocks and flux of these organisms, it is important to standardize the sampling strategy.

A polar study (Meilland et al., 2018) has reported planktic foraminiferal standing stocks of 205.05–618.9 μg m^{-3} and flux of 25.16–92.03 mg m^{-2} day^{-1} along the southern Polar Front (between 50 and 60°S). Recently, it has been reported that Arctic foraminiferal shells are heavier (containing more calcite) and thicker than the specimens inhabiting the Antarctic and Sub-Antarctic sector (Schiebel et al., 2017). However, the average foraminiferal shell weights estimated from the northern Svalbard margin reported in our study (on average 6.68 μg from the 250–500 μm size fraction and 2.22 μg from the 100–250 μm size fraction) agrees well with the shell weights reported from the Sub-Antarctic (Meilland et al., 2018). Nevertheless, the difference on the mesh size used to sample [100 μm in Meilland et al. (2018)] could influence the size distribution, collecting larger individuals and, therefore, likely heavier individuals. We combine the weight of 257 planktic foraminiferal specimens following the equations published in Meilland et al. (2018). These equations, based on specimens from the sub-Antarctic, lead to an estimated mass of 6.77 μg (250–500 μm), 1.71 μg (100–250 μm), and 0.46 (90–100 μm). Hence, we might be inducing just a negligible bias on our estimates.

In case of the shelled pteropods, Bednaršek et al. (2012a) reviewed published abundance and biomass data from all over the world. Abundances of 10.87 and 18.52 ind m^{-3} from veligers (250–500 μm) and adults of *L. helicina* with an associated biomass of 0.27 and 11.11 mg m^{-3}, respectively, were reported in the Northern Barents Sea (Blachowiak-Samolyk et al., 2008). Highest values were recorded over the Western Svalbard margin while the lowest values were obtained closer to our sampling area. However, those values are difficult to compare because of the different mesh size used [90 μm in our study compared to 180 μm in Blachowiak-Samolyk et al. (2008)].

Ocean Acidification Perspectives

The Arctic Ocean in general is expected to be a 'hotspot' of ocean acidification (Orr et al., 2005; Sugie et al., 2020). Indeed, Chierici et al. (2019) estimated continued CO_2 uptake by the ocean at the West Spitsbergen shelf and on the slope north of Svalbard. With the effect of ocean acidification, the planktic foraminifera and pteropods shells are expected to be more fragile, to produce thinner and smaller shells, require more energy to clacify, and to be prone to dissolution (Moy et al., 2009; Bednaršek et al., 2012b; Manno et al., 2018). Lower shell weights and, therefore, lower test sinking velocity associated with each size fraction, could result in decreased carbonate standing stocks and export production from these marine calcifiers. The impact of ocean acidification to their calcification process and the lower export of their inorganic shells to the sea floor are expected to alter the carbonate compensation depth in the near future and, when less of these shells dissolve, decrease the carbonate ion concentration on the longer term [Middelburg et al. (2020) and references therein]. Ultimately, a decrease in sinking velocity, would affect the inorganic carbon pump turning it less effective (Bednaršek et al., 2014). Experiments show that exposing *L. helicina antarctica* to an aragonite saturation state (Ω_{AR}) of 0.8 for 100 days, would reduce the shell weight by half and reduce its sinking velocity proportionally [Bednaršek et al. (2014) and references therein]. A previous experiment reported that ocean acidification would decrease the terminal sinking velocity of the subpolar *L. retroversa* after being maintained at medium (800 μatm) and high (1200 μatm) controlled levels of CO_2 (Bergan et al., 2017). *Limacina retroversa* is more able to tolerate wider ranges of temperature (2.0–7.0°C) and salinity (30.1–36.0) than *L. helicina*, thus the former species could have more chance to survive in a warning climate than the latter (Manno et al., 2012).

Pteropods with shells built of aragonite, are more susceptible to dissolution than organisms with shells of calcite, and are expected to be more vulnerable toward changes in the seawater carbonate chemistry. Due to their high vulnerability and contribution to the inorganic standing stocks and productivity, ocean acidification might have considerable and unpredicted effects on the standing stocks and export production in the northern Svalbard shelf and Arctic deep basin.

CONCLUSION

In the northern Barents Sea and Svalbard margin, the vertical distribution patterns of planktic foraminifera and shelled pteropods, not affected by diurnal vertical migration, show a clear depth zonation. Large (>500 μm) and medium sized (250–500 μm) pteropods dominate in the upper 50 m of the water column. In general, no pteropods were found below 100 m depth. Both medium sized (100–250 μm) and

small sized (90–100 μm) foraminifera dominate from 50 to 300 m depth. The foraminiferal community is dominated by the polar species *Neogloboquadrina pachyderma* (33–67%), the subpolar species *Turborotalita quinqueloba* (6–32%) and *Neogloboquadrina incompta* (8–34%). The pteropod community is largely dominated by *Limacina helicina* (>94.2%). Based on our data we attribute the increase in subpolar species of foraminifera (*N. incompta* and *T. quinqueloba*) and pteropods (*L. retroversa*) to the "Atlantification" process.

Despite their lower abundance, the estimated contribution of shelled pteropods to late summer inorganic carbon standing stocks and export production drastically exceeds the contribution of planktic foraminifera. The inorganic standing stocks and export production from pteropods represent 66.6–96.5 and 56.7–98−4% of the total inorganic carbon, respectively. The organic standing stocks and export production from pteropods, represent 75.0 – 97.5 and 67.4–99.1% of the total organic carbon, respectively. The sensitivity of their shells toward changes in the environment should be considered when predicting how ocean acidification might affect the carbonate standing stocks and fluxes. Due to the lack of seasonal sampling, it is difficult to estimate the pelagic production, budgets and fluxes that would reflect the annual variability.

The combined potential effect of ocean acidification and "Atlantification" in the Barents Sea remains poorly understood. "Atlantification" processes could lead to a dominance of subpolar species, higher abundances and productivity and larger shells. In contrast, ocean acidification is expected to make the shells of calcifiers more fragile and affect their growth, thus reducing their contribution to the inorganic carbon cycle. In the future one could therefore expect that subpolar species increase their relative abundance, but decrease their shell thickness and size, since subpolar species might be less adapted to low pH.

DATA AVAILABILITY STATEMENT

The raw data supporting the conclusion of this article will be made available by the authors, without undue reservation.

AUTHOR CONTRIBUTIONS

GA-O analyzed the plankton samples, calculated standing stocks and production, and drafted the manuscript. TR contributed with cruise data, samples and finances, and original research plan. The study was designed by TR, GA-O, PZ, KZ, and JM. KZ contributed to the species identification. JM and PZ contributed to the standing stocks and production part of the study. JM contributed to the statistical analyses. MC and AF performed the carbonate chemistry analyses. The manuscript was finalized with contributions from GA-O, KZ, JM, PZ, MC, AF, and TR. All authors contributed to the article and approved the submitted version.

FUNDING

The study was carried out as part of the Research Council of Norway through the project "The Nansen Legacy" (RCN #276730) and partly within the framework of the Flagship research program "Ocean Acidification and effects in northern waters" within the FRAM – High North Research Centre for Climate and the Environment at the Norwegian Polar Institute, Norway. This work was also supported by the Centre for Arctic Gas Hydrate, Environment and Climate (CAGE), the Research Council of Norway through its Centers of Excellence scheme (Grant #223259) and CALMED (#CTM2016-79547-R) projects of the Spanish Ministry of Science and Innovation, and the Generalitat de Catalunya MERS (#2017 SGR-1588).

ACKNOWLEDGMENTS

We are grateful to the captain and crew from RV Helmer Hansen and all cruise participants, especially S. Ofstad and N. El bani Altuna for collecting the samples. We also thank the AMGG (Arctic Marine Geology and Geophysics) Research School for supporting the cruise.

SUPPLEMENTARY MATERIAL

The Supplementary Material for this article can be found online at: https://www.frontiersin.org/articles/10.3389/fmars.2021.661158/full#supplementary-material

REFERENCES

Akiha, F., Hashida, G., Makabe, R., Hattori, H., and Sasaki, H. (2017). Distribution in the abundance and biomass of shelled pteropods in surface waters of the Indian sector of the Antarctic Ocean in mid-summer. *Polar Sci.* 12, 12–18. doi: 10.1016/j.polar.2017.02.003

Anderson, L. G., and Macdonald, R. W. (2015). Observing the Arctic Ocean carbon cycle in a changing environment. *Polar Res.* 34:26891. doi: 10.3402/polar.v34.26891

Årthun, M., Eldevik, T., Smedsrud, L., Skagseth, Ø, and Ingvaldsen, R. (2012). Quantifying the influence of Atlantic heat on Barents Sea ice variability and retreat. *J. Clim.* 25, 4736–4743. doi: 10.1175/jcli-d-11-00466.1

Bates, N., and Mathis, J. (2009). The Arctic Ocean marine carbon cycle: evaluation of air-sea CO 2 exchanges, ocean acidification impacts and potential feedbacks. *Biogeosciences* 6, 2433–2459. doi: 10.5194/bg-6-2433-2009

Bauch, D., Erlenkeuser, H., Winckler, G., Pavlova, G., and Thiede, J. (2002). Carbon isotopes and habitat of polar planktic foraminifera in the Okhotsk Sea: the 'carbonate ion effect'under natural conditions. *Mar. Micropaleontol.* 45, 83–99. doi: 10.1016/s0377-8398(02)00038-5

Bauch, H. A. (1999). "Planktic foraminifera in Holocene sediments from the Laptev Sea and the Central Arctic Ocean: species distribution and paleobiogeographical implication," in *Land-Ocean Systems in the Siberian Arctic*, eds H. Kassens, H. A. Bauch, I. A. Dmitrenko, H. Eicken, H.-W. Hubberten, M. Melles et al. (Berlin: Springer), 601–613. doi: 10.1007/978-3-642-60134-7_46

Bednaršek, N., Feely, R. A., Howes, E. L., Hunt, B. P., Kessouri, F., León, P., et al. (2019). Systematic review and meta-analysis toward synthesis of thresholds of ocean acidification impacts on calcifying pteropods and interactions with warming. *Front. Mar. Sci.* 6:227. doi: 10.3389/fmars.2019.00227

Bednaršek, N., Možina, J., Vogt, M., O'brien, C., and Tarling, G. (2012a). The global distribution of pteropods and their contribution to carbonate and carbon biomass in the modern ocean. *Earth Syst. Sci. Data* 4, 167–186. doi: 10.5194/essd-4-167-2012

Bednaršek, N., Tarling, G., Bakker, D., Fielding, S., Jones, E., Venables, H., et al. (2012b). Extensive dissolution of live pteropods in the Southern Ocean. *Nat. Geosci.* 5, 881–885. doi: 10.1038/ngeo1635

Bednaršek, N., Tarling, G. A., Bakker, D. C., Fielding, S., Cohen, A., Kuzirian, A., et al. (2012c). Description and quantification of pteropod shell dissolution: a sensitive bioindicator of ocean acidification. *Glob. Change Biol.* 18, 2378–2388. doi: 10.1111/j.1365-2486.2012.02668.x

Bednaršek, N., Tarling, G. A., Bakker, D. C., Fielding, S., and Feely, R. A. (2014). Dissolution dominating calcification process in polar pteropods close to the point of aragonite undersaturation. *PLoS One* 9:e109183. doi: 10.1371/journal.pone.0109183

Beer, C. J., Schiebel, R., and Wilson, P. A. (2010). Technical note: on methodologies for determining the size-normalised weight of planktic foraminifera. *Biogeosciences* 7, 2193–2198. doi: 10.5194/bg-7-2193-2010

Bergan, A. J., Lawson, G. L., Maas, A. E., and Wang, Z. A. (2017). The effect of elevated carbon dioxide on the sinking and swimming of the shelled pteropod *Limacina retroversa*. *ICES J. Mar. Sci.* 74, 1893–1905. doi: 10.1093/icesjms/fsx008

Bjørklund, K. R., Kruglikova, S. B., and Anderson, O. R. (2012). Modern incursions of tropical Radiolaria into the Arctic Ocean. *J. Micropalaeontol.* 31, 139–158. doi: 10.1144/0262-821x11-030

Blachowiak-Samolyk, K., Søreide, J. E., Kwasniewski, S., Sundfjord, A., Hop, H., Falk-Petersen, S., et al. (2008). Hydrodynamic control of mesozooplankton abundance and biomass in northern Svalbard waters (79–81 N). *Deep Sea Res. 2 Top. Stud. Oceanogr.* 55, 2210–2224. doi: 10.1016/j.dsr2.2008.05.018

Bluhm, B., Kosobokova, K., and Carmack, E. (2015). A tale of two basins: an integrated physical and biological perspective of the deep Arctic Ocean. *Progr. Oceanogr.* 139, 89–121. doi: 10.1016/j.pocean.2015.07.011

Buitenhuis, E., Vogt, M., Moriarty, R., Bednarsek, N., Doney, S. C., Leblanc, K., et al. (2013). MAREDAT: towards a world atlas of MARine Ecosystem DATa. *Earth Syst. Sci. Data* 5, 227–239. doi: 10.5194/essd-5-227-2013

Buitenhuis, E. T., Le Quere, C., Bednaršek, N., and Schiebel, R. (2019). Large contribution of Pteropods to shallow CaCO3 export. *Glob. Biogeochem. Cycles* 33, 458–468. doi: 10.1029/2018gb006110

Carstens, J., Hebbeln, D., and Wefer, G. (1997). Distribution of planktic foraminifera at the ice margin in the Arctic (Fram Strait). *Mar. Micropaleontol.* 29, 257–269. doi: 10.1016/s0377-8398(96)00014-x

Carstens, J., and Wefer, G. (1992). Recent distribution of planktonic foraminifera in the Nansen Basin, Arctic Ocean. *Deep Sea Res. A. Oceanogr. Res. Papers* 39, S507–S524.

Chang, Y., and Yen, J. (2012). Swimming in the intermediate reynolds range: kinematics of the pteropod *Limacina helicina*. *Integr. Comp. Biol.* 52, 597–615. doi: 10.1093/icb/ics113

Chierici, M., and Fransson, A. (2018). "Arctic chemical oceanography at the edge: focus on carbonate chemistry (chapter 13)", in *At the Edge*, ed. P. Wassmann, 343.

Chierici, M., Vernet, M., Fransson, A., and Børsheim, K. Y. (2019). Net community production and carbon exchange from winter to summer in the Atlantic water inflow to the Arctic Ocean. *Front. Mar. Sci.* 6:528. doi: 10.3389/fmars.2019.00528

Davis, C. V., Rivest, E. B., Hill, T. M., Gaylord, B., Russell, A. D., and Sanford, E. (2017). Ocean acidification compromises a planktic calcifier with implications for global carbon cycling. *Sci. Rep.* 7:2225.

Descamps, S., Aars, J., Fuglei, E., Kovacs, K. M., Lydersen, C., Pavlova, O., et al. (2017). Climate change impacts on wildlife in a High Arctic archipelago–Svalbard, Norway. *Glob. Change Biol.* 23, 490–502. doi: 10.1111/gcb.13381

Dickson, A. (1990). Standard potential of the (AgCl (s)+ 1/2H2 (g)= Ag (s)+ HCl (aq)) cell and the dissociation constant of bisulfate ion in synthetic sea water from 273.15 to 318.15 K. *J. Chem. Thermodyn.* 22, 113–127. doi: 10.1016/0021-9614(90)90074-z

Dickson, A., and Millero, F. J. (1987). A comparison of the equilibrium constants for the dissociation of carbonic acid in seawater media. *Deep Sea Res. A Oceanogr. Res. Papers* 34, 1733–1743. doi: 10.1016/0198-0149(87)90021-5

Dickson, A. G., Sabine, C. L., and Christian, J. R. (2007). *Guide to Best Practices for Ocean CO2 Measurements*. Sydney, VIC: North Pacific Marine Science Organization.

Drits, A., Klyuvitkin, A., Kravchishina, M., Karmanov, V., and Novigatsky, A. (2020). Fluxes of sedimentary material in the lofoten basin of the Norwegian Sea: seasonal dynamics and the role of zooplankton. *Oceanology* 60, 501–517. doi: 10.1134/s0001437020040074

Fabry, V. J. (1989). Aragonite production by pteropod molluscs in the subarctic Pacific. *Deep Sea Res. A Oceanogr. Res. Papers* 36, 1735–1751. doi: 10.1016/0198-0149(89)90069-1

Fabry, V. J. (2008). Marine calcifiers in a high-CO2 ocean. *Science* 320, 1020–1022. doi: 10.1126/science.1157130

Fabry, V. J., Seibel, B. A., Feely, R. A., and Orr, J. C. (2008). Impacts of ocean acidification on marine fauna and ecosystem processes. *ICES J. Mar. Sci.* 65, 414–432. doi: 10.1093/icesjms/fsn048

Falk-Petersen, S., Leu, E., Berge, J., Kwasniewski, S., Nygård, H., Røstad, A., et al. (2008). Vertical migration in high Arctic waters during autumn 2004. *Deep Sea Res. 2 Top. Stud. Oceanogr.* 55, 2275–2284. doi: 10.1016/j.dsr2.2008.05.010

Fox, L., Stukins, S., Hill, T., and Miller, C. G. (2020). Quantifying the effect of anthropogenic climate change on calcifying plankton. *Sci. Rep.* 10:1620.

Greco, M., Jonkers, L., Kretschmer, K., Bijma, J., and Kucera, M. (2019). Depth habitat of the planktonic foraminifera *Neogloboquadrina pachyderma* in the northern high latitudes explained by sea-ice and chlorophyll concentrations. *Biogeosciences* 16, 3425–3437. doi: 10.5194/bg-16-3425-2019

Guinotte, J. M., and Fabry, V. J. (2008). Ocean acidification and its potential effects on marine ecosystems. *Ann. N. Y. Acad. Sci.* 1134, 320–342. doi: 10.1196/annals.1439.013

Hop, H., Assmy, P., Wold, A., Sundfjord, A., Daase, M., Duarte, P., et al. (2019). Pelagic ecosystem characteristics across the Atlantic water boundary current from Rijpfjorden, Svalbard, to the Arctic Ocean during summer (2010-2014). *Front. Mar. Sci.* 6:181. doi: 10.3389/fmars.2019.00181

Husum, K., and Hald, M. (2012). Arctic planktic foraminiferal assemblages: implications for subsurface temperature reconstructions. *Mar. Micropaleontol.* 96, 38–47. doi: 10.1016/j.marmicro.2012.07.001

Jonkers, L., Hillebrand, H., and Kucera, M. (2019). Global change drives modern plankton communities away from the pre-industrial state. *Nature* 570, 372–375. doi: 10.1038/s41586-019-1230-3

Kacprzak, P., Panasiuk, A., Wawrzynek, J., and Weydmann, A. (2017). Distribution and abundance of pteropods in the western Barents Sea. *Oceanol. Hydrobiol. Stud.* 46:393. doi: 10.1515/ohs-2017-0039

Katz, M. E., Cramer, B. S., Franzese, A., Hönisch, B.r, Miller, K. G., Rosenthal, Y., et al. (2010). Traditional and emerging geochemical proxies in foraminifera. *J. Foraminifer. Res.* 40, 165–192. doi: 10.2113/gsjfr.40.2.165

Kohfeld, K. E., Fairbanks, R. G., Smith, S. L., and Walsh, I. D. (1996). *Neogloboquadrina pachyderma* (sinistral coiling) as paleoceanographic tracers in polar oceans: evidence from Northeast Water Polynya plankton tows, sediment traps, and surface sediments. *Paleoceanography* 11, 679–699. doi: 10.1029/96pa02617

Kolås, E. H., Koenig, Z., Fer, I., Nilsen, F., and Marnela, M. (2020). Structure and transport of Atlantic Water north of Svalbard from observations in summer and fall 2018. *J. Geophys. Res. Oceans* 125:e2020JC016174.

Lalli, C. M., and Gilmer, R. W. (1989). *Pelagic Snails: the Biology of Holoplanktonic Gastropod Mollusks*. Stanford, CA: Stanford University Press.

Langer, M. R. (2008). Assessing the Contribution of Foraminiferan Protists to Global Ocean Carbonate Production 1. *J. Eukaryot. Microbiol.* 55, 163–169. doi: 10.1111/j.1550-7408.2008.00321.x

Lee, K., Kim, T.-W., Byrne, R. H., Millero, F. J., Feely, R. A., and Liu, Y.-M. (2010). The universal ratio of boron to chlorinity for the North Pacific and North Atlantic oceans. *Geochim. Cosmochim. Acta* 74, 1801–1811. doi: 10.1016/j.gca.2009.12.027

Lee, Y. J., Matrai, P. A., Friedrichs, M. A., Saba, V. S., Antoine, D., Ardyna, M., et al. (2015). An assessment of phytoplankton primary productivity in the

Arctic Ocean from satellite ocean color/in situ chlorophyll−a based models. *J. Geophys. Res. Oceans* 120, 6508–6541. doi: 10.1002/2015jc011018

Lischka, S., and Riebesell, U. (2012). Synergistic effects of ocean acidification and warming on overwintering pteropods in the Arctic. *Glob. Change Biol.* 18, 3517–3528. doi: 10.1111/gcb.12020

Manno, C., Bednaršek, N., Tarling, G. A., Peck, V. L., Comeau, S., Adhikari, D., et al. (2017). Shelled pteropods in peril: assessing vulnerability in a high CO2 ocean. *Earth Sci. Rev.* 169, 132–145. doi: 10.1016/j.earscirev.2017.04.005

Manno, C., Giglio, F., Stowasser, G., Fielding, S., Enderlein, P., and Tarling, G. (2018). Threatened species drive the strength of the carbonate pump in the northern Scotia Sea. *Nat. Commun.* 9:4592.

Manno, C., Morata, N., and Primicerio, R. (2012). *Limacina retroversa*'s response to combined effects of ocean acidification and sea water freshening. *Estuar. Coast. Shelf Sci.* 113, 163–171. doi: 10.1016/j.ecss.2012.07.019

Manno, C., and Pavlov, A. (2014). Living planktonic foraminifera in the Fram Strait (Arctic): absence of diel vertical migration during the midnight sun. *Hydrobiologia* 721, 285–295. doi: 10.1007/s10750-013-1669-4

Mehrbach, C., Culberson, C., Hawley, J., and Pytkowicx, R. (1973). Measurement of the apparent dissociation constants of carbonic acid in seawater at atmospheric pressure 1. *Limnol. Oceanogr.* 18, 897–907. doi: 10.4319/lo.1973.18.6.0897

Meilland, J., Howa, H., Hulot, V., Demangel, I., Salaun, J., and Garlan, T. (2020). Population dynamics of modern planktonic foraminifera in the western Barents Sea. *Biogeosciences* 17, 1437–1450. doi: 10.5194/bg-17-1437-2020

Meilland, J., Schiebel, R., Monaco, C. L., Sanchez, S., and Howa, H. (2018). Abundances and test weights of living planktic foraminifers across the Southwest Indian Ocean: implications for carbon fluxes. *Deep Sea Res.2 Oceanogr. Res. Papers* 131, 27–40. doi: 10.1016/j.dsr.2017.11.004

Meyer, A., Sundfjord, A., Fer, I., Provost, C., Villacieros Robineau, N., Koenig, Z., et al. (2017). Winter to summer oceanographic observations in the Arctic Ocean north of Svalbard. *J. Geophys. Res. Oceans* 122, 6218–6237. doi: 10.1002/2016jc012391

Middelburg, J. J., Soetaert, K., and Hagens, M. (2020). Ocean alkalinity, buffering and biogeochemical processes. *Rev. Geophys.* 58:e2019RG000681.

Millero, F. J. (1979). Effects of pressure and temperature on activity coefficients. *Act. Coefficients Electrolyte Solututions* 2, 63–151.

Moy, A. D., Howard, W. R., Bray, S. G., and Trull, T. W. (2009). Reduced calcification in modern Southern Ocean planktonic foraminifera. *Nat. Geosci.* 2, 276–280. doi: 10.1038/ngeo460

Mucci, A. (1983). The solubility of calcite and aragonite in seawater at various salinities, temperatures, and one atmosphere total pressure. *Am. J. Sci.* 283, 780–799. doi: 10.2475/ajs.283.7.780

NOAA NCFEI. (2018). *Climate at a Glance: Global Mapping* [Online]. Available online at: https://www.ncdc.noaa.gov/snow-and-ice/extent/ (accessed May 13, 2021).

Ofstad, S., Meilland, J., Zamelczyk, K., Chierici, M., Fransson, A., Gründger, F., et al. (2020). Development, productivity, and seasonality of living planktonic foraminiferal faunas and *Limacina helicina* in an Area of intense methane seepage in the Barents Sea. *J. Geophys. Res. Biogeosci.* 125: e2019JG005387.

Onarheim, I. H., Smedsrud, L. H., Ingvaldsen, R. B., and Nilsen, F. (2014). Loss of sea ice during winter north of Svalbard. *Tellus A Dyn. Meteorol. Oceanogr.* 66:23933. doi: 10.3402/tellusa.v66.23933

Orr, J. C., Fabry, V. J., Aumont, O., Bopp, L., Doney, S. C., Feely, R. A., et al. (2005). Anthropogenic ocean acidification over the twenty-first century and its impact on calcifying organisms. *Nature* 437, 681–686. doi: 10.1038/nature04095

Pados, T., and Spielhagen, R. F. (2014). Species distribution and depth habitat of recent planktic foraminifera in Fram Strait. Arctic Ocean. *Polar Res.* 33, 22483. doi: 10.3402/polar.v33.22483

Peck, V. L., Oakes, R. L., Harper, E. M., Manno, C., and Tarling, G. A. (2018). Pteropods counter mechanical damage and dissolution through extensive shell repair. *Nat. Commun.* 9:264.

Pierrot, D., Lewis, E., and Wallace, D. (2006). *MS Excel Program Developed for CO2 System Calculations*. Oak Ridge, TN: Oak Ridge National Laboratory, 10.

Renner, A., Sundfjord, A., Janout, M., Ingvaldsen, R. B., Beszczynska−Möller, A., Pickart, R. S., et al. (2018). Variability and redistribution of heat in the Atlantic water boundary current north of Svalbard. *J. Geophys. Res. Oceans* 123, 6373–6391. doi: 10.1029/2018jc013814

Riley, J., and Tongudai, M. (1967). The major cation/chlorinity ratios in sea water. *Chem. Geol.* 2, 263–269. doi: 10.1016/0009-2541(67)90026-5

Roy, T., Lombard, F., Bopp, L., and Gehlen, M. (2015). Projected impacts of climate change and ocean acidification on the global biogeography of planktonic Foraminifera. *Biogeosciences* 12, 2873–2889. doi: 10.5194/bg-12-2873-2015

Sakshaug, E. (1997). Biomass and productivity distributions and their variability in the Barents Sea. *ICES J. Mar. Sci.* 54, 341–350. doi: 10.1006/jmsc.1996.0170

Salter, I., Schiebel, R., Ziveri, P., Movellan, A., Lampitt, R., and Wolff, G. A. (2014). Carbonate counter pump stimulated by natural iron fertilization in the Polar Frontal Zone. *Nat. Geosci.* 7, 885–889. doi: 10.1038/ngeo2285

Schiebel, R. (2002). Planktic foraminiferal sedimentation and the marine calcite budget. *Glob. Biogeochem. Cycles* 16, 3-1-3-21.

Schiebel, R., Barker, S., Lendt, R., Thomas, H., and Bollmann, J. (2007). Planktic foraminiferal dissolution in the twilight zone. *Deep Sea Res. 2 Top. Stud. Oceanogr.* 54, 676–686. doi: 10.1016/j.dsr2.2007.01.009

Schiebel, R., and Hemleben, C. (2000). Interannual variability of planktic foraminiferal populations and test flux in the eastern North Atlantic Ocean (JGOFS). *Deep Sea Res. 2 Top. Stud. Oceanogr.* 47, 1809–1852. doi: 10.1016/s0967-0645(00)00008-4

Schiebel, R., Spielhagen, R. F., Garnier, J., Hagemann, J., Howa, H., Jentzen, A., et al. (2017). Modern planktic foraminifers in the high-latitude ocean. *Mar. Micropaleontol.* 136, 1–13. doi: 10.1007/978-3-662-50297-6_1

Schneider, C. A., Rasband, W. S., and Eliceiri, K. W. (2012). NIH Image to ImageJ: 25 years of image analysis. *Nat. Methods* 9, 671–675. doi: 10.1038/nmeth.2089

Shadwick, E., Trull, T., Thomas, H., and Gibson, J. (2013). Vulnerability of polar oceans to anthropogenic acidification: comparison of Arctic and Antarctic seasonal cycles. *Sci. Rep.* 3:2339.

Simstich, J., Sarnthein, M., and Erlenkeuser, H. (2003). Paired δ18O signals of *Neogloboquadrina pachyderma* (s) and *Turborotalita quinqueloba* show thermal stratification structure in Nordic Seas. *Mar. Micropaleontol.* 48, 107–125. doi: 10.1016/s0377-8398(02)00165-2

Sugie, K., Fujiwara, A., Nishino, S., Kameyama, S., and Harada, N. (2020). Impacts of temperature, CO2, and salinity on phytoplankton community composition in the Western Arctic Ocean. *Front. Mar. Sci.* 6:821. doi: 10.3389/fmars.2019.00821

Sundfjord, A., Assmann, K. M., Lundesgaard, Ø, Renner, A. H. H., Lind, S., and Ingvaldsen, R. B. (2020). *Suggested Water Mass Definitions for the Central and Northern Barents Sea, and the Adjacent Nansen Basin: Workshop Report.", in: The Nansen Legacy Report Series 8/2020*. Tromsø: The Nansen Legacy.

Takahashi, K., and Bé, A. (1984). Planktonic foraminifera: factors controlling sinking speed. *Deep Sea Res. A Oceanogr. Res. Papers* 31, 1477–1500. doi: 10.1016/0198-0149(84)90083-9

Volkmann, R. (2000). Planktic foraminifers in the outer Laptev Sea and the Fram Strait—Modern distribution and ecology. *J. Foraminifer. Res.* 30, 157–176. doi: 10.2113/0300157

Wassmann, P., Slagstad, D., and Ellingsen, I. H. (2019). Advection of Mesozooplankton into the Northern svalbard shelf region. *Front. Mar. Sci.* 6:458. doi: 10.3389/fmars.2019.00458

Weinkauf, M. F., Kunze, J. G., Waniek, J. J., and Kučera, M. (2016). Seasonal variation in shell calcification of planktonic foraminifera in the NE Atlantic reveals species-specific response to temperature, productivity, and optimum growth conditions. *PLoS One* 11:e0148363. doi: 10.1371/journal.pone.0148363

Zamelczyk, K., Rasmussen, T. L., Raitzsch, M., and Chierici, M. (2020). The last two millennia: climate, ocean circulation and palaeoproductivity inferred from planktic foraminifera, south-western Svalbard margin. *Polar Res.* 39. doi: 10.33265/polar.v39.3715

Ziveri, P., de Bernardi, B., Baumann, K.-H., Stoll, H. M., and Mortyn, P. G. (2007). Sinking of coccolith carbonate and potential contribution to organic carbon ballasting in the deep ocean. *Deep Sea Research Part II: Topical Studies in Oceanography* 54, 659–675. doi: 10.1016/j.dsr2.2007.01.006

Conflict of Interest: The authors declare that the research was conducted in the absence of any commercial or financial relationships that could be construed as a potential conflict of interest.